ADIABATIC DEMAGNETIZATION

ADIABATIC DEMAGNETIZATION

By

HOWARD JOHN ORANGE LAWRENCE, B.Eng.

A Thesis

Submitted to the Faculty of Graduate Studies

in Partial Fulfilment of the Requirements

for the Degree

Master of Engineering

McMaster University

May 1965

MASTER OF ENGINEERING (1965)
(Electrical)

McMaster University,
Hamilton, Ontario.

Title: Adiabatic Demagnetization

Author: Howard John Orange Lawrence, B.Eng. (McMaster University)

Supervisor: Professor C.K. Campbell

Number of Pages: v, 55

Scope and Contents:

The construction of an adiabatic demagnetization cryostat has been outlined in detail along with the associated electrical apparatus for supplying power to the cryostat and for temperature measurement. Various magnet electrical configurations have been suggested and tried, and the degree of success of each noted.

Two types of working coolants, Ferric Ammonium Sulphate and Pink Ruby have been considered and the advantages and disadvantages of each have been discussed. Suggestions for further improvements have also been made.

ABSTRACT

We have investigated the construction of a low temperature source based on the principle of adiabatic demagnetization. A superconducting solenoid has been used successfully as the source of magnetic field and the possibility of using a circulating superconducting current in the solenoid has met with limited success. Temperature was determined by measuring the magnetic susceptibility using an electronic Hartshorn bridge and relating it to temperature by Curie's law. With this apparatus a temperature of 0.35 degree Kelvin was reached using pink ruby as the magnetic material.

ACKNOWLEDGEMENTS

The author wishes to express his gratitude for the continued advice and encouragement received from Dr. C.K. Campbell. For a summer grant and most of the instruments which made this investigation possible, the author is deeply indebted to the National Research Council.

TABLE OF CONTENTS

INTRODUCTION

1.1 Problem of a Low Temperature Source

The liquification of helium by Kammerlingh Onnes in 1908 marks the last stage of reaching low temperatures by liquification of a gas because helium is the last element to remain in the gaseous state when the temperature is decreased. The temperature of liquid helium under 1 atmosphere of its own vapour is 4.2°K. With a reasonably moderate pumping system, the faster molecules of liquid Helium may be pumped off leaving liquid at a temperature in the range of 1.0°K - 1.2°K. With more elaborate, expensive pumping and special techniques, temperatures of about 0.7°K. are possible. This is the lowest temperature achieved by this method. If it is necessary to investigate material below this temperature, a new source of heat extraction will have to be found.

Several means of reaching lower temperatures has been proposed. The most expensive, no doubt, is the liquification of a rare isotope of helium with an atomic weight of 3. This isotope must be produced by nuclear reactors to obtain large enough quantities for liquifying, but by means of pumping on the vapour of this liquid, it is possible to reach temperatures of 0.3°K.

The most appealing method from an economic standpoint, however, is quite different and it is the one that has been attempted.

1.2 Proposed Solution

Consider a system of energy states of a particle such as a molecule in a solid. Each state is represented by a horizontal line as in Fig. 1.

The shaded area on each state represents the number of particles in each of these states and this number is a function of the Boltzman distribution: $\exp[-E/kT]$ where E is the energy of each state, T is the absolute temperature and k the Boltzman constant. Consider now an external parameter X which varies the energy of each level. If we change the parameter from X_1 to X_2 thereby increasing the energy gap between each level, we would have the situation existing as shown in Fig. 1(b). We have, however, by raising the energy levels and maintaining the population of these levels, raised the energy of total system. The increase of energy appears as an increase in temperature. If we now allow this energy to escape in the form of heat until the original temperature is reached, we have the original distribution of particles appearing again in Fig. 1(c), but populating different energy states. The external parameter is now changed from X_2 to X_1 thereby compressing other energy levels as shown in Fig. 1(d). If no exchange of energy in the form of heat is permitted with the surroundings, then the distribution of particles as shown in Fig. 1(d) corresponds to a lower temperature given by a new Boltzman distribution $\exp(-E/kT_2)$, where T_2 is the new temperature. The new temperature is lower than the temperature we started with in Fig. 1(a).

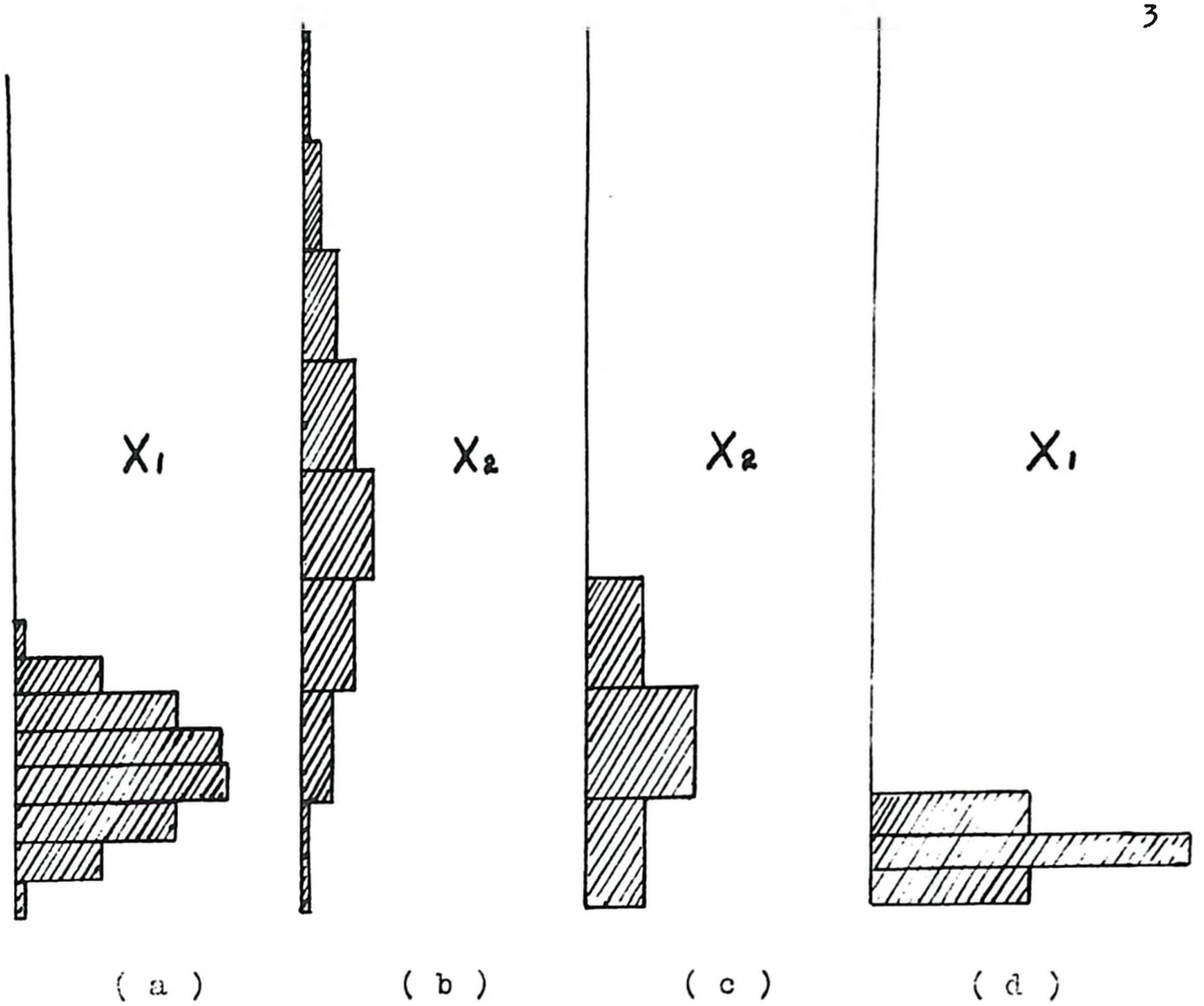

Figure 1. Energy of a given state as a function of population.

This theory was put to practical use in 1923[2] when Kammerlingh Onnes and Woltjer carried out experiments on the magnetic properties of gadolinium sulphate. The found that over a particular range of temperatures, for example, centered about 1°K., the magnetic dipoles showed no dependence on temperature, that is, the thermal energy kT was much larger than the energy differences between states shown in Fig. 1.

This led Debye[3] and Giauque[4] to suggest independently that perhaps a source of low temperatures would be a magnetic material, fulfilling the requirements as depicted in Fig. 1. In this case, the external parameter would be a magnetic field.

However, it was not until 1933 that Giauque and McDougall[5] in Berkeley, California, and de Haas, Wierema, and Kramers[6] in Leiden, Holland, attempted to use this method. In each case, the magnets used to provide the external field consumed a great deal of power and either the magnet (in the case of an iron core), or the power-supply (in the case of an iron-free solenoid) was unwieldy. For example, the magnet used at the Kammerlingh Onnes laboratory for this type of experiment contains 12 tons of iron.[7]

Subsequent removal of the iron magnet was also very difficult because it was necessary to move either the very heavy iron mass or elaborate pumping lines and dewars from the iron mass.

In 1961, Kropschot and Arp[8] performed this experiment using a solenoid wound of superconducting wire. Since a transformer is required for the measurement of temperature, they also suggested using the solenoid for the primary of this transformer. This arrangement has the ad-

vantage that the magnet producing the magnetic field does not have to be removed from the apparatus. Since the wire of the solenoid is superconducting, it also means that a relatively insignificant power supply is required compared to what was formerly required.

In all of the experiments mentioned above, there is one common characteristic that we will also use, that is, all the experimental apparatus is cooled in a bath of liquid helium at 4.2°K. followed by use of a large rotary pump which cools this liquid to approximately 1.2°K.

This experiment is a construction of an apparatus which cools other material to temperatures below 1.2°K. in order that we may measure their properties in this range of temperatures. Furthermore, we require a method for measuring temperatures with reasonable accuracy.

THEORY OF ADIABATIC DEMAGNETIZATION

2.1

Requirements of Material

The magnetic system required for this experiment is a type known as Paramagnetic, that is, its magnetic properties are derived from the moments of the electrons spinning about their axes. The Pauli Exclusion Principle, however, requires that the ion in question has an odd number of orbiting electrons in order that it may have a net magnetic moment.

Furthermore, let us consider the susceptibility of the paramagnetic material.

For a paramagnetic material, the susceptibility varies inversely with the temperature as shown in Fig. 2 where curve (a) is represented by the equation:

$$\chi = C/T \tag{1}$$

Where X is the susceptibility, C the Curie constant and T, the absolute temperature, this is known as Curie's Law. Curve (b) is a more general representation and has the equation:

$$\chi = C/(T - \theta) \tag{2}$$

Where θ is the Curie (Neel) temperature, this is known as the Curie-Weiss Law.

When the very low temperature portion of this curve is used for adiabatic demagnetization, it is necessary to use the more exact Curie-Weiss Law to interpret the data. In our apparatus, however, we propose to

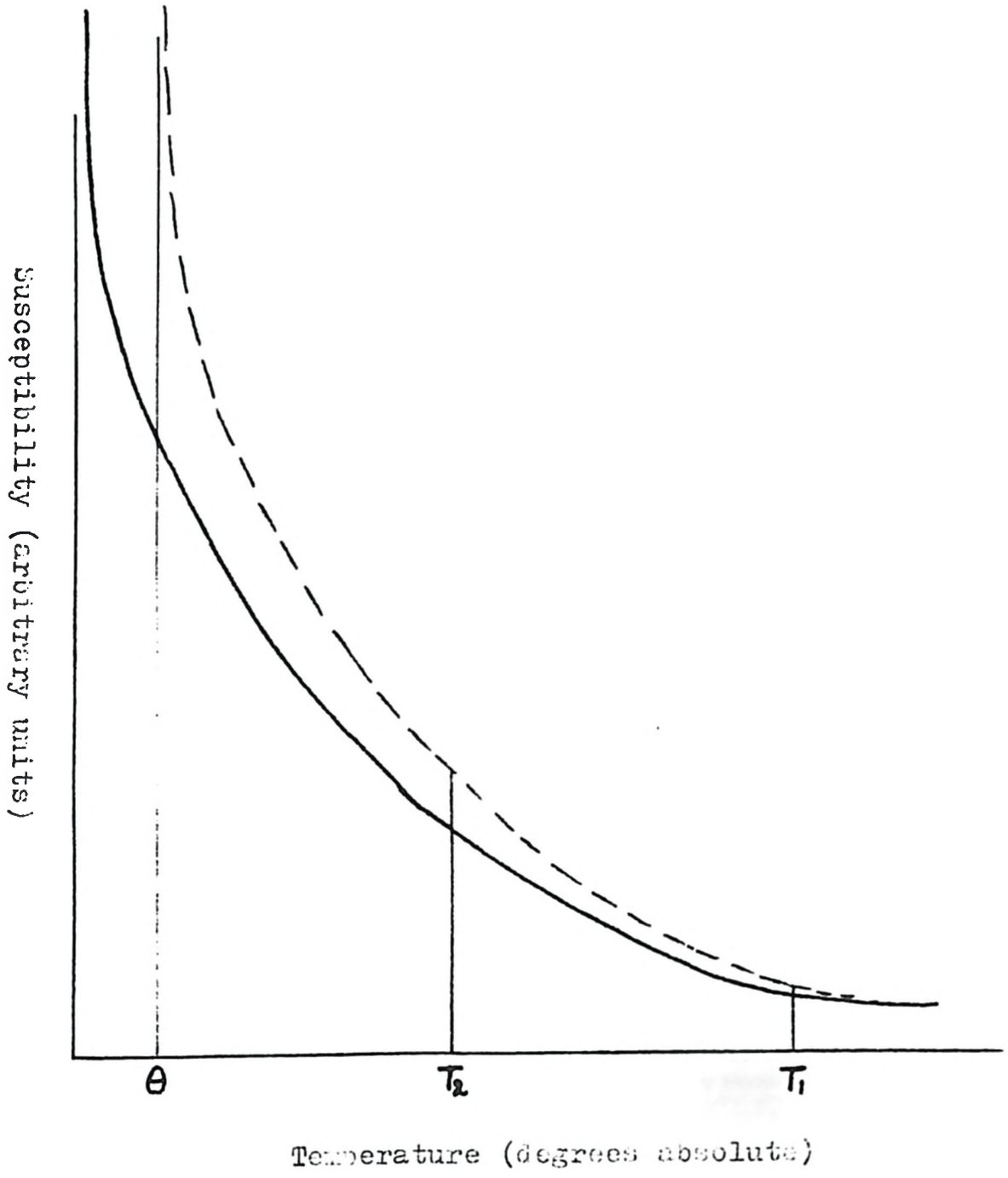

(a) ——— Curie Law

(b) - - - - Curie-Weiss Law

Figure 2. Susceptibility as a function of Temperature.

use the temperature region above T_2 on the curve where the simple Curie Law is sufficiently exact to adequately explain the results.

The next requirement of the paramagnetic material is that the energy level splittings and broadenings due to the interaction forces of the ions must be small compared to kT (the thermal energy, where k is the Boltzman Constant) at 1°K. The energy difference between the levels should also be the same order of magnitude as kT at 1°K. in a magnetic field of a few thousand gauss.(9)

If we represent the difference between the energy states by the relation, $g\beta H$, where g represents the spectroscopic splitting, β represents the Bohr magnetron and H is the applied field, it is desirable to have

$$g\beta H > kT$$

for H in the order of a few thousand gauss, to facilitate observations.

There are several dilute salts that fulfil these requirements. If we now choose T_1 (on Fig. 2) as our starting temperature, we see that the Curie temperature Θ (in order of 0.06°K.)(10) is very small compared to T_1 and consequently justifies our using the Curie Law instead of the Curie-Weiss law.

2.2.

Magnetic Cooling

First let us consider a pictorial diagram of adiabatic demagnetization in order to understand the thermodynamic relationships developed later.

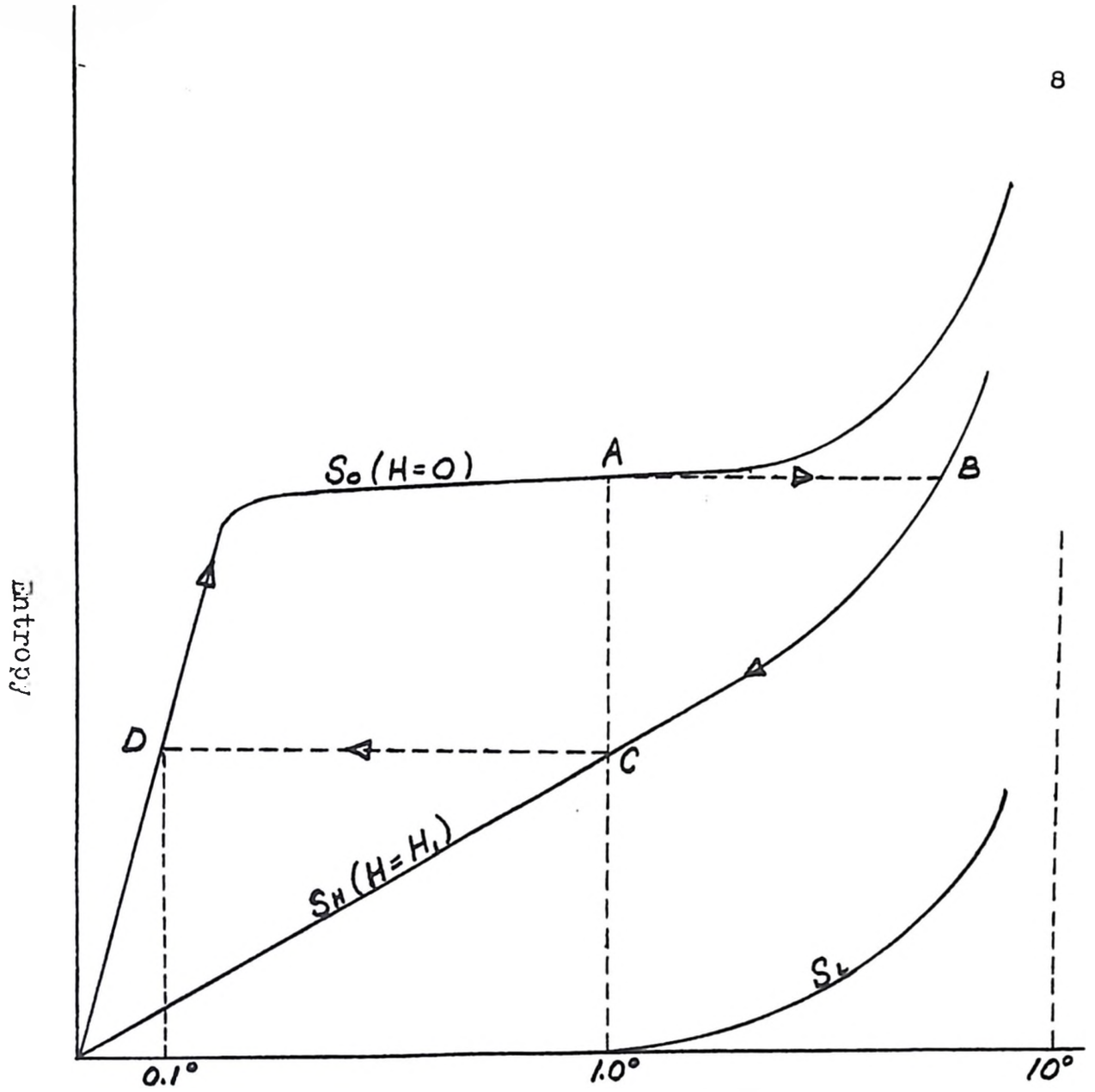

Figure 3. Entropy as a function of Temperature.

In Fig. 3, we have plotted three curves of entropy against temperature. The uppermost represents the entropy of a paramagnetic system of spins with no applied magnetic field. The high temperature end of this curve rises sharply due to the sharp increase in lattice entropy in this region - which in turn is a result of thermal vibration. The center portion of the curve corresponds to an ideal paramagnetic gas, i.e. the paramagnetic ion energies are quite small compared to kT. No alignment occurs until in the region of approximately 0.1°K. where the ions align themselves and consequently result in a decrease of the entropy of the spin system. Curve S_h on the other hand, represents the entropy of the spin system in a high magnetic field. We now see that the magnetic field has increased the spin energy level (Zeeman splittings) until they are the same order of magnitude as kT. As can be seen in this diagram, the ordering is more linearly dependent on the temperature.

Curve S_L represents the entropy of the lattice and is only a small fraction of the entropy in the temperature range of interest. This also indicates that because there is a large portion of the remaining entropy due to the magnetic spin system, this should be a good means to provide a lower temperature.

A typical procedure would be to start at point A on this diagram, i.e. the paramagnetic system would be at approximately 1°K. (in zero field). The temperature would be maintained by some type of thermal contact between the paramagnetic material and the surrounding liquid helium bath kept at 1°K. The first step would be to magnetize the material in a field of a few thousand gauss. Magnetization of the spin system, like

the compression of a gas, liberates heat which we wish to conduct to the liquid helium bath. Ideally, we wish to reach point C on the high field curve and the shortest possible route is along the line of isothermal magnetization AC. This, however, involves slowly increasing the applied field in order that the paramagnetic material remains in thermal equilibrium with the temperature bath. Fortunately, this time consuming step is not necessary. It is much easier to simply turn the field on to maximum value than to wait for thermal equilibrium to be reached with each incremental change of field.

In turning the field on, it reaches its maximum value before any significant heat can be conducted to the temperature bath. This step follows an isentropic change (along AB) to the high field curve. At point B, the spin system has considerably more energy than 1°K. so the thermal contact conducts this heat to the bath and the material follows the high field curve from point B to C in cooling down. At point C, we have the material at 1°K. in a high magnetic field and consequently strongly magnetized. If we quickly remove the magnetic field, we return to the zero field at some point between points D and A. If very severe heat leaks exist, the material returns to point A along CA and no cooling is achieved. If, however, reasonably good thermal isolation is possible, the material will cool adiabatically to point D and the example will show a significant decrease in temperature. In practice, a reasonable heat leak is on the order of one erg. per second. In order that this process is most efficient, it must be done reversibly, that is, as the spin system is cooled, it must cool the lattice with it and not remain as local cold

regions in a warm lattice for the heat capacity at 1°K. is still appreciable. Thus we require a spin-lattice relaxation time that is not so long that the lattice absorbs heat from outside the apparatus faster than the spin system draws energy from it. For most spin systems this relaxation time appears to be less than one second[12] and should not lead to any gross irreversibilities in this process since the applied field is generally regulated to zero in some time greater than one second.

From point D on the zero field curve, the material increases in temperature along DA until point A is reached.

The thermodynamic relations for each of these steps are worked out in the next section.

2.3 Thermodynamic Relationships

The thermodynamic basis for magnetic cooling may be shown by starting with the relationship:[13]

$$\begin{aligned} dU' &= TdS - MdH \\ dU &= TdS + HdH \end{aligned} \qquad (1)$$

$$U = U' + MH$$

dU represents the change in internal free energy, S is the entropy, H is theapplied field and M is the magnetic moment of the magnetized field. MH is the term representing the presence of the magnetic material and field simultaneously. All terms of the general thermodynamic relationship for free energy concerning non-magnetic work (e.g. pdv) have been

omitted because they are usually negligible in magnetic considerations and certainly in the temperature range below 1°K.[9]

Applying the condition that S is a total differention to equation (1), we see:

$$\begin{aligned} C_m dT &= T dS + T\left(\frac{\partial H}{\partial T}\right)_m \times dM \\ C_h dT &= T dS - T\left(\frac{\partial M}{\partial T}\right)_h \times dH \end{aligned} \qquad (2)$$

C_m and C_h are the specific heats for constant magnetic moment and constant field and are:

$$C_h = T\left(\frac{\partial S}{\partial T}\right)_h \quad \text{and} \quad C_m = T\left(\frac{\partial S}{\partial T}\right)_m$$

Solving for C_h and C_m from equation (2)

$$C_h = C_m - T\left(\frac{\partial M}{\partial T}\right)_h \cdot \left(\frac{\partial H}{\partial T}\right)_m$$

Now using Curie's Law which states:

$$M = \frac{CH}{T} \qquad (3)$$

where C is Curie's constant, we obtain the relation:

$$C_h = C_m + \frac{CH^2}{T^2}$$

Furthermore, if we combine equations (1) and (2), we obtain the relation:

$$\left(\frac{\partial T}{\partial H}\right)_S = -\left(\frac{\partial H}{\partial S}\right)_H \qquad (4)$$

i.e. the rate of change of temperature with magnetic field for an isentropic change is equal to the negative rate of change of magnetic moment with entropy at a constant field.

From equation (2), we use an isentropic process (ds = 0) to produce cooling:

$$ChdT = -T\left(\frac{\partial M}{\partial T}\right)_h \times dH$$

For a paramagnetic material (M/ T)h which is negative then a negative dH implies a negative dT and the final temperature T_f is found by the integration of equation (4):

$$T_f - T_o = -\int_{H_o}^{H_f} \left(\frac{\partial M}{\partial S}\right)_h \cdot dH \qquad (5)$$

where T_o, H_o are the initial temperature and fields and H_f is the final field.

Consider the change of magnetic moment with field and temperature is an isentropic process. Applying a small field H, first isothermally then adabatically to a paramagnetic material initially at temperature T, will give two magnetic moments M(H, T) and M(H, T') respectively, where T' is the temperature in the magnetic field.

The difference will be:

$$M(H,T) - M(H,T') = \left(\frac{\partial M}{\partial T}\right)_h (T' - T)$$

or

$$M(H,T) - M(H,T') = -\left(\frac{\partial M}{\partial T}\right)_h \cdot \int_0^H \left(\frac{\partial M}{\partial S}\right)_h \cdot dH$$

by substitution of equation (5).

Using Curie's Law (equation 3), we can show the curves of isothermal and adiabatic magnetization are related as:

$$\left(\frac{\partial M\,(H,\,T)}{\partial H}\right)_S \;\text{——}\; \left(\frac{\partial M\,(H,\,T)}{\partial H}\right)_t = \left(\frac{\partial M}{\partial T}\right)_h \times \left(\frac{\partial T}{\partial H}\right)_S$$

$$= -\left(\frac{\partial M}{\partial T}\right)_h \times \left(\frac{\partial M}{\partial S}\right)_h \qquad (7)$$

by substitution of equation (4).

Since both of the last terms equal zero when H = 0, we can assume that both these curves have equal slopes in zero field. However, these curves when started from a zero field temperature will have a differentiate in a finite field that may be approximated by:

$$\frac{\partial^2 M}{\partial T\,\partial H}\,(T' - T) = -\frac{\partial^2 M}{\partial T\,\partial H}\int_0^h \left(\frac{\partial M}{\partial S}\right)_h \cdot dH \text{ by equation (5)}$$

Substituting into equation (7) we now have our relation for the magnetic moment for an isentropic process, i.e.:

$$\left(\frac{\partial M(H,T')}{\partial H}\right)_S - \left(\frac{\partial M(H,T)}{\partial H}\right)_T = -\left(\frac{\partial M}{\partial T}\right)_H \times \left(\frac{\partial M}{\partial S}\right)_H$$

$$-\frac{\partial^2 M}{\partial H\,\partial T}\int_0^h \left(\frac{\partial M}{\partial S}\right)_H \cdot dH$$

The change of entropy during the process of isothermal magnetization may be found by integration of equation (2)[14] where dT = 0

$$So - S = \int_0^H \left(\frac{\partial M}{\partial T}\right)_T \cdot dH \qquad (8)$$

So is the entropy of the system before the magnetization process started and S is the entropy after magnetization. This difference in entropy must be equal to the difference in entropy between the initial temperation and the final lowest temperature achieved by subsequently removing the magnetic field from the system, i.e.

$$\int_0^{M(H,T)} \left(\frac{\partial H}{\partial T}\right)_M \cdot dM = \int_{T_1}^{T} \frac{Co}{T}\, dT = -\int_0^{H_1} \left(\frac{\partial M}{\partial T}\right)_T \cdot dH \qquad (9)$$

where Co is the zero field specific heat of the paramagnetic material. Therefore by starting at a finite temperature with any material we are able to measure the heat input for any amount of cooling and plot a curve of susceptibility vs. temperature.

Having laid the theoretical foundation for each of the steps outlined in the beginning of this section, we will now proceed to the physical solution of each of these steps.

TEMPERATURE MEASUREMENT

3.1 Temperature vs. Susceptibility

As we approach these low temperatures, the problem of temperature measurement becomes paramount. The only remaining "gas" at these temperatures is the vapour pressure of liquid helium itself. For example, the vapour pressure of liquid helium at 1.0°K is 0.1205[15] mm. Hg. or 2×10^{-4} atm. and at 0.1°K, it is 10^{-32} mm. The gas thermometer becomes useless in this region. However, as we have mentioned earlier, materials best suited for adiabatic demagnetization experiments are those that most closely obey Curie's Law ($X = C/T$) down to the lowest temperature. For this reason, one might be tempted to base absolute temperature determination on this law. In these experiments, the sample under investigation may be the coolant and also the thermometer.[16] Hence the gas thermometer with the "perfect gas" should be replaced by a "perfect paramagnetic material" and the temperature should be derived from the measured susceptibility as:

$$T = C \frac{H}{M} = C/X$$

However, because of the increasing magnetic ion interaction as the temperature decreases, no material can obey Curie's law down to absolute zero, consequently corrections must be applied to our thermometer much the same as are applied to a gas thermometer.

Thus, C/X is not the absolute temperature but a quantity related to it by the true magnetic equation of state of the material under investigation. Since a susceptibility measurement can be easily performed C/X is a very suitable thermometric parameter and is called the "magnetic temperature". Then:

$$T^* = C \frac{H}{M} = C/X$$

where T^* is the magnetic temperature.

The relation between the true temperature and the magnetic temperature T^* may be found experimentally.[17] This is done by demagnetizing the same sample from the same temperature Ti but in fields of different magnitudes as shown in figure 4.

Since the absolute temperature Ti is known, the entropy difference $S_1 - S_2$, (ΔS) corresponding to values of the field H_1 and H_2 can be determined. Now demagnetizing adiabatically to H = 0 gives us temperatures, T_1^* and T_2^* and we can directly measure the heat input required to raise the temperature of the sample from T_2^* to T_1^*. Hence the average final temperature $T_{1,2}$ can be fixed in the absolute scale by the relation $Q = T\Delta S$. By carrying out a number of experiments from close values of H at T_1, a continuous T^*, T relation (where T is the absolute temperature) may be established for this particular material.

Close to 1°K, the magnetic temperature is practically equal to the thermodynamic temperature for this particular sample and the difference becomes more and more significant with decreasing temperature as shown on the graph of Fig. 5.

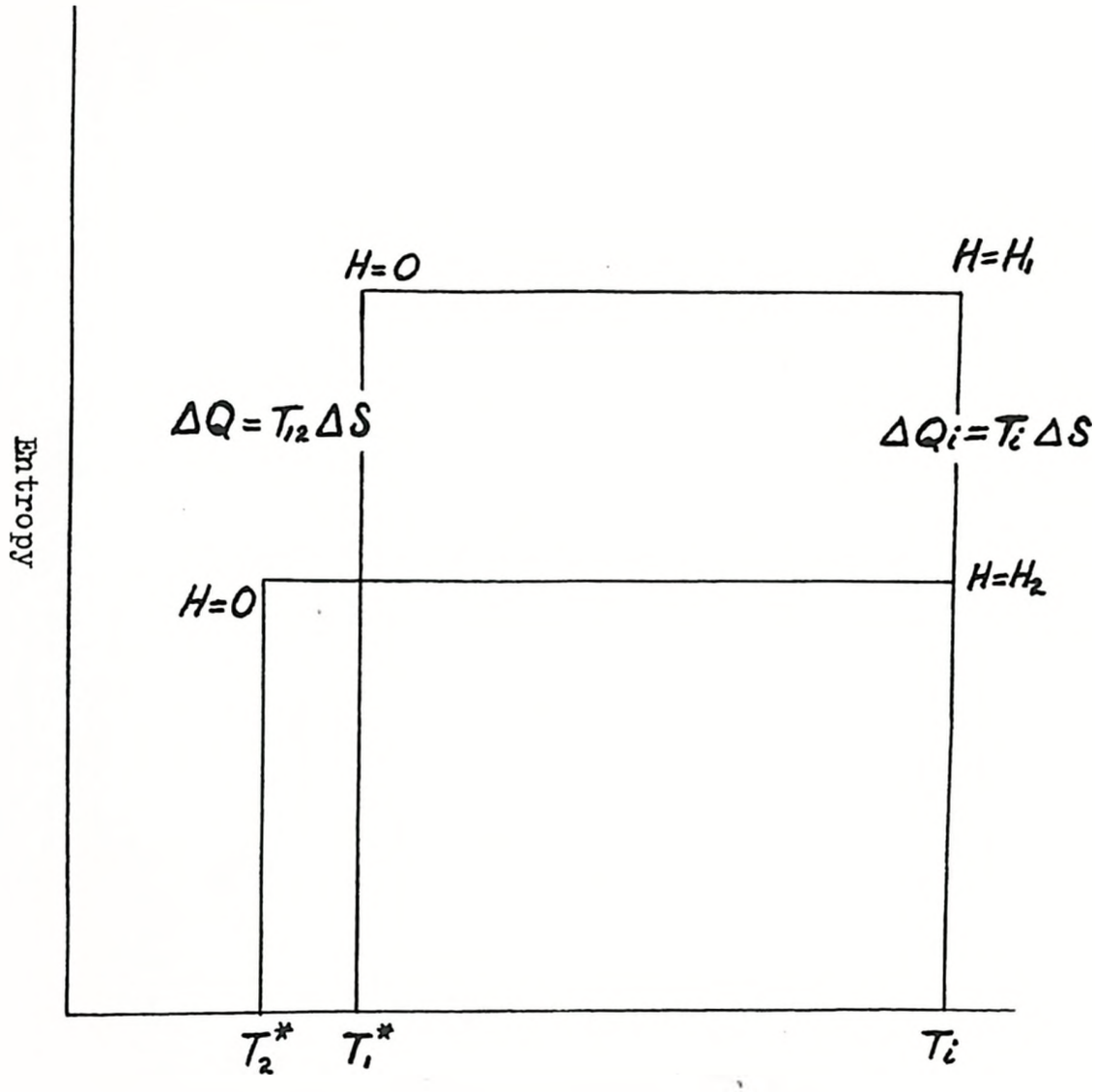

Figure 4. Entropy as a function of Temperature.

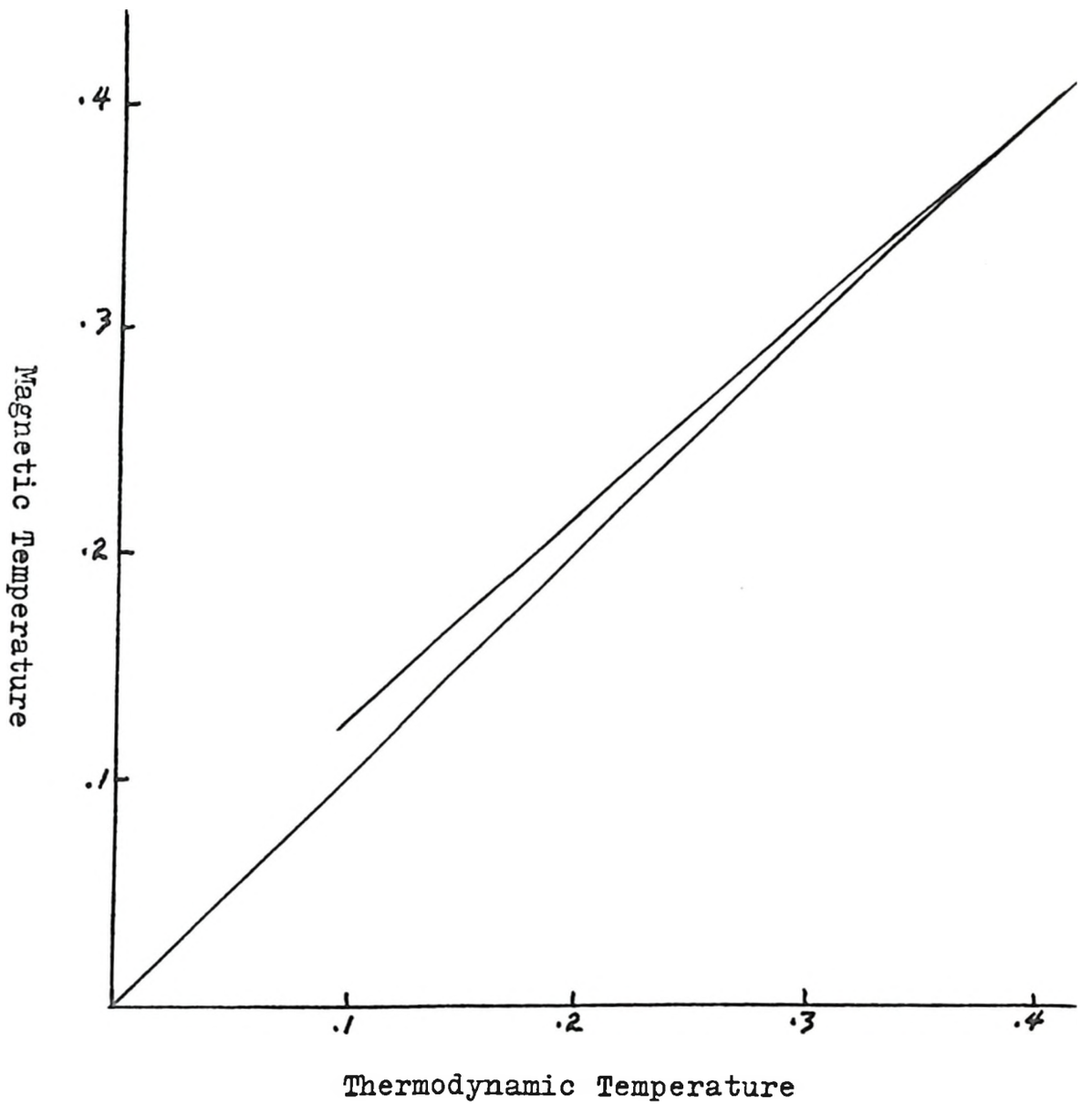

Figure 5. Magnetic Temperature as a function of Thermodynamic Temperature.

3.2 Mutual Inductance Bridge

Since we are now able to relate the susceptibility of a material to its temperature, our problem now becomes one of measuring the susceptibility. This susceptibility is measured on an alternating current Hartshorn bridge[19], an instrument that will measure the mutual inductance between two coils and is shown in simplified form in Fig. 6.

Coil M_1, consists of two concentric coils - a primary and a secondary with the sample of material in the coil. M_2 consists of two coils in which we may vary the coupling between them and this mutual coupling is calibrated in henries. Coils M_1 and M_2 are wound inopposition.

We assume the susceptibility of the material may be divided into two components:

$$X = X' - iX''$$

where X' is the in phase component and X'' is the lossy component. If our bridge is now balanced we find:

$$M_1 = M_o + C\,(X' - iX'')$$

where M_o is the mutual inductance with no paramagnetic present and C is a geometric factor. We see now that M_2 can only balance the $M_o + CX'$ portion of M_1, since they both give rise to voltages in quadrature with the primary current. The voltage due to CX'' is in phase with the primary current and hence can be balanced by setting the potentiometer R. The balance conditions can thus be written as:

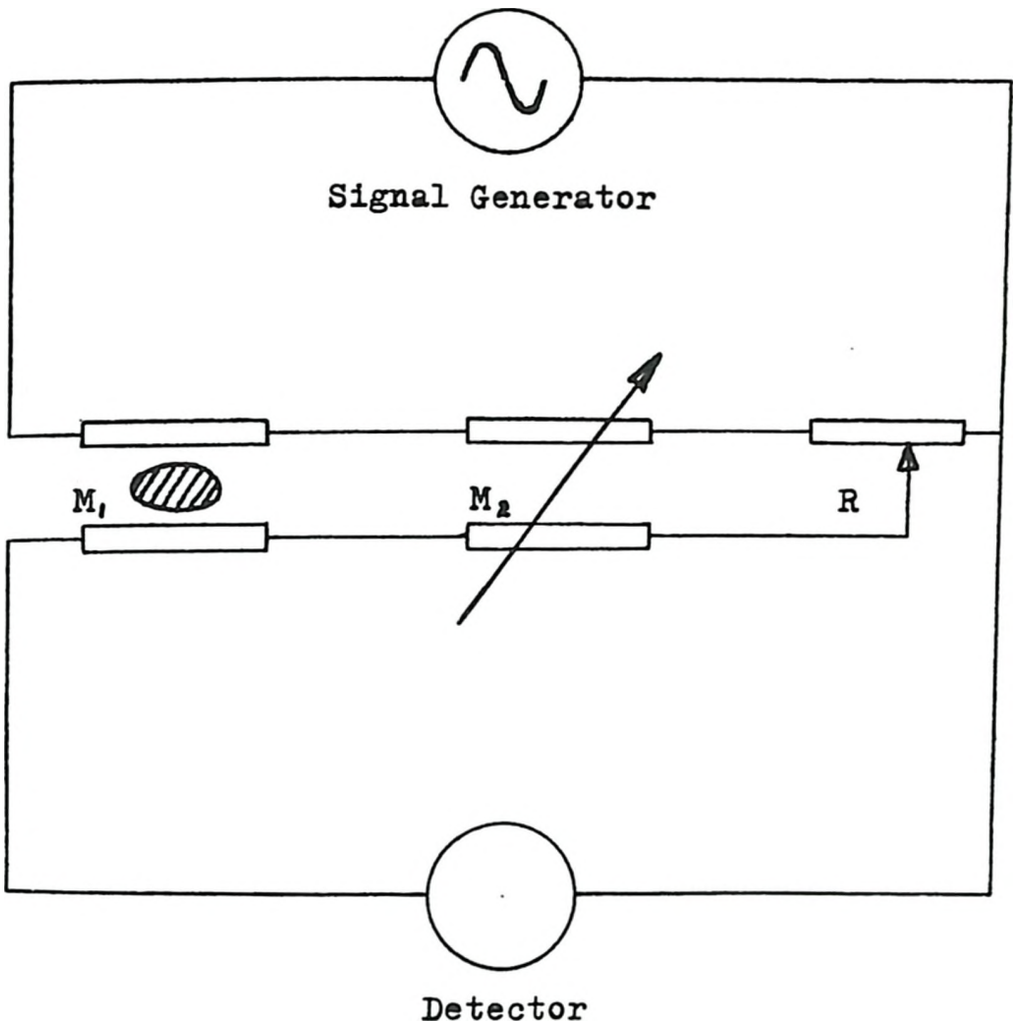

Figure 6. Alternating Current Hartshorn Bridge.

$$M_2 = M_o + CX' \qquad (1)$$

$$R = CWX'' \qquad (2)$$

where W is the angular frequency of the signal generator.

As a result of the small value of the susceptibility of a paramagnetic material, a great deal of care is required in measuring this mutual inductance. This has been achieved by using the electronic bridge (Cryotronics, type ML155B) shown in figure 7.[20] Here the measuring coils are again denoted M_1 but note the secondary is astatically wound thus decreasing the term M_o in equation (1) and consequently increasing the relative magnitude of the susceptibility term CX'. By astatically winding this coil, we have also reduced the pickup of external magnetic noise. The signal generator, transformer, coupled with the primary circuit provides a primary current which passes through a decade resistor p. The resistor p and the triode tube form an artificial primary circuit feeding the fixed mutual inductor m. The Bridge is balanced by adjusting the value of p_1, thereby adjusting the a.c. current i_m in the primary of m and hence the induced voltage in the secondary of M_2. This circuit gives constant primary and secondary impedances, a much desired feature, and also allows decade resistors to take the place of decade mutual inductors.

The triode plate resistance is very large in comparison with the circuit reactance and the a.c. current i_m is in phase with the applied signal voltage $i_p p$. For a tube of transconductance g, we have

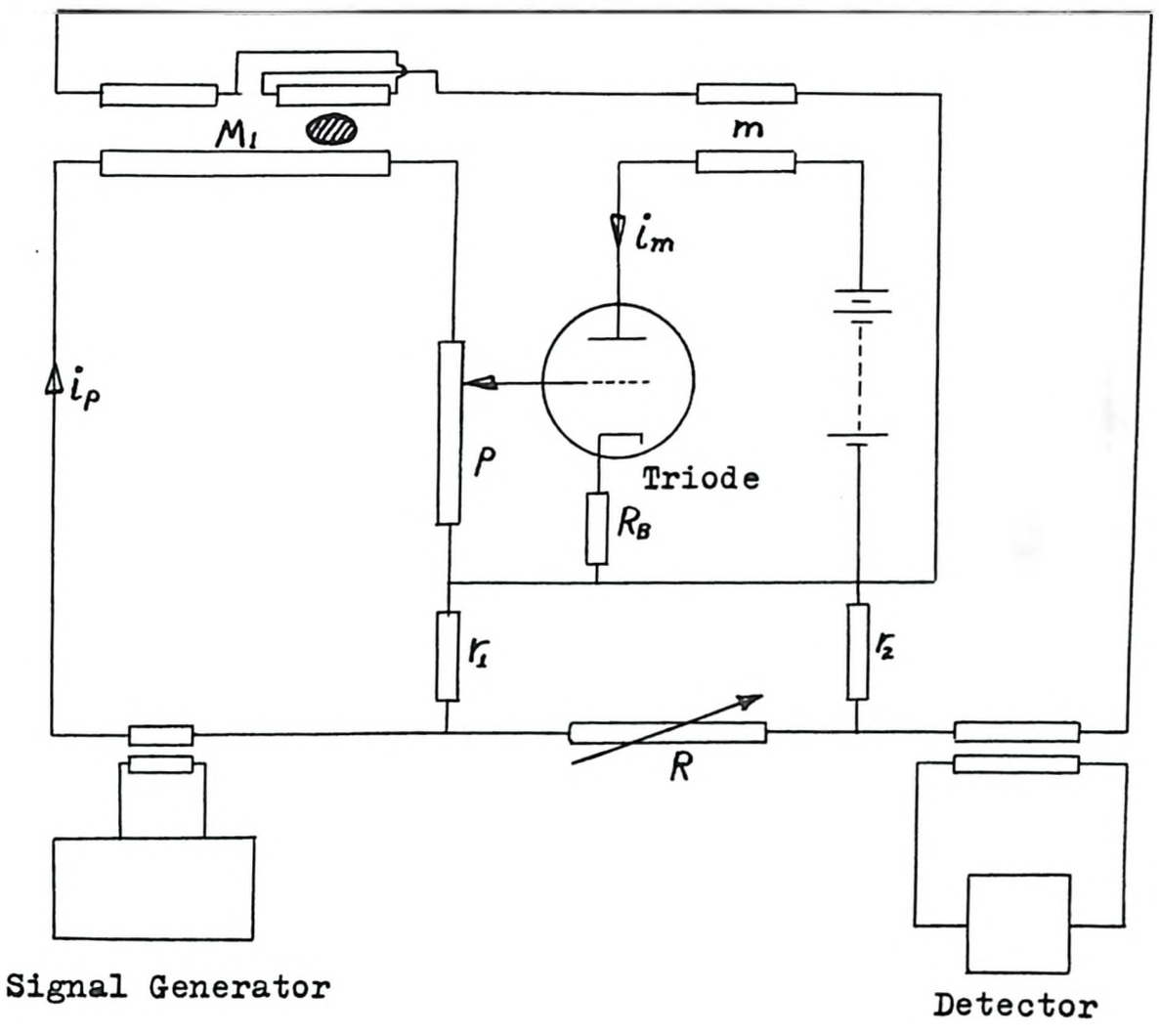

Figure 7. Electronic Mutual Inductance Bridge.

$$i_m = pGi_p/(1 + gR_B) = pGi \qquad (3)$$

where R_B is the bias resistor and G is the effective transconductance. The mutual inductance M_2 then induces a signal into the secondary circuit which is given by

$$V_m = j\omega M i_m = j\omega(pMG)i_p \qquad (4)$$

The resistance network r_1, r_2, and R has an equivalent resistance R_e where

$$R_e = r_1 r_2/(R+r_1+r_2)$$

such that it introduces a voltage $R_e i_p$ into the secondary circuit. This network balances any lossy component in the test mutual M_1.

When we compare equation 4 to equation 1

$$M_2 = M_o + CX' \qquad (1)$$

$$pMG = \text{Constant} + M \qquad (4)$$

we see that a variation in susceptibility X' corresponds to a variation of M in (4) and this in turn is measured by a change in p. Therefore, p may be calibrated in units of inductance.

To measure temperature we must plot the mutual inductance against the inverse temperature in the liquid helium range between 4.2°K and 1.2°K. The temperature in this range can be found very accurately by measuring the vapour pressure of the liquid helium bath and using the prepared tables[15] for relating it to temperature. By projecting this susceptibility graph to higher values of inductance we are able to relate higher readings of mutual inductance to temperatures below 1°K for as long as Curie's law remains accurate.

Such a method requires a new calibration curve for each experiment since it is difficult to obtain the same high temperature mutual, but the simplicity of the calibration curve more than anything else warrants its use.

DESCRIPTION OF APPARATUS

4.1 Low Temperature Chamber

The experimental chamber is shown in detail in figure 8 with ruby used as the paramagnetic material. This ruby is supported by a nylon cup which has been necked to reduce the possibility of heat leaks[21]. The nylon support is in turn held in place by a glass tube projecting from the bottom of the experimental chamber. This much of the apparatus is shown also in figure 9. Figure 9 also shows aluminum foil which was glued to the outside of the chamber in an effort to further reduce heat leaks. The scale of this picture may be determined when it is known the ruby is two inches in length and 0.25" in diameter.

This bottom is sealed to the rest of the chamber by a ground glass joint and the entire chamber is suspended from a high vacuum pumping line. The thermodynamic relationships are now met by permitting helium gas at 10^{-3} mm to enter the chamber down the pumping tube to provide thermal contact with the liquid helium bath. Similarly, the thermal contact is broken by pumping out this exchange gas with a high vacuum pump. The interior of the chamber is silvered, as is the pumping tube, to reduce heat leaks. The tube is also provided with a few kinks and bends (radiation traps) to prevent radiation from "light-piping" down the tube. This radiation trap is shown in figure 10.

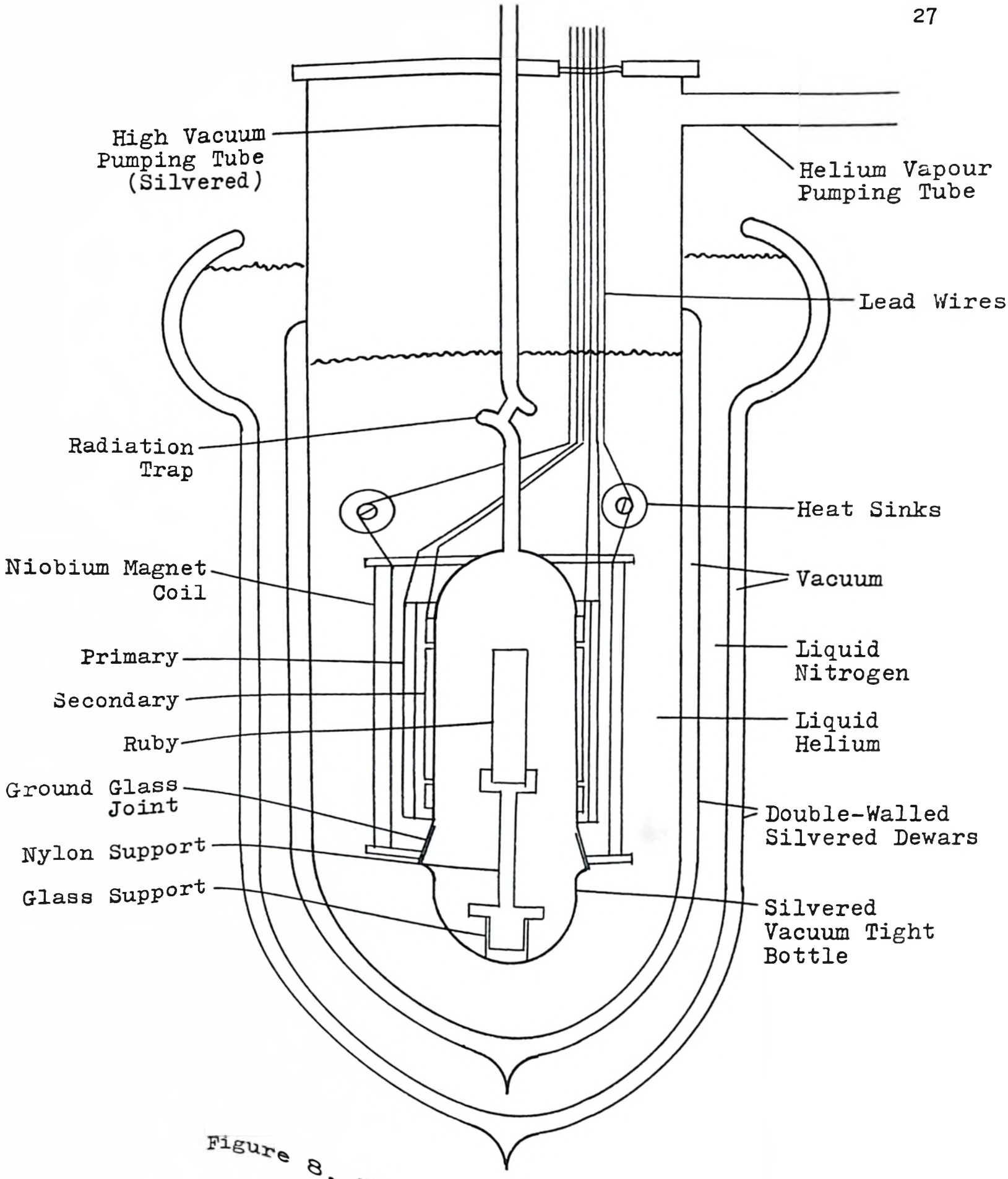

Figure 8. Experimental Cryostat.

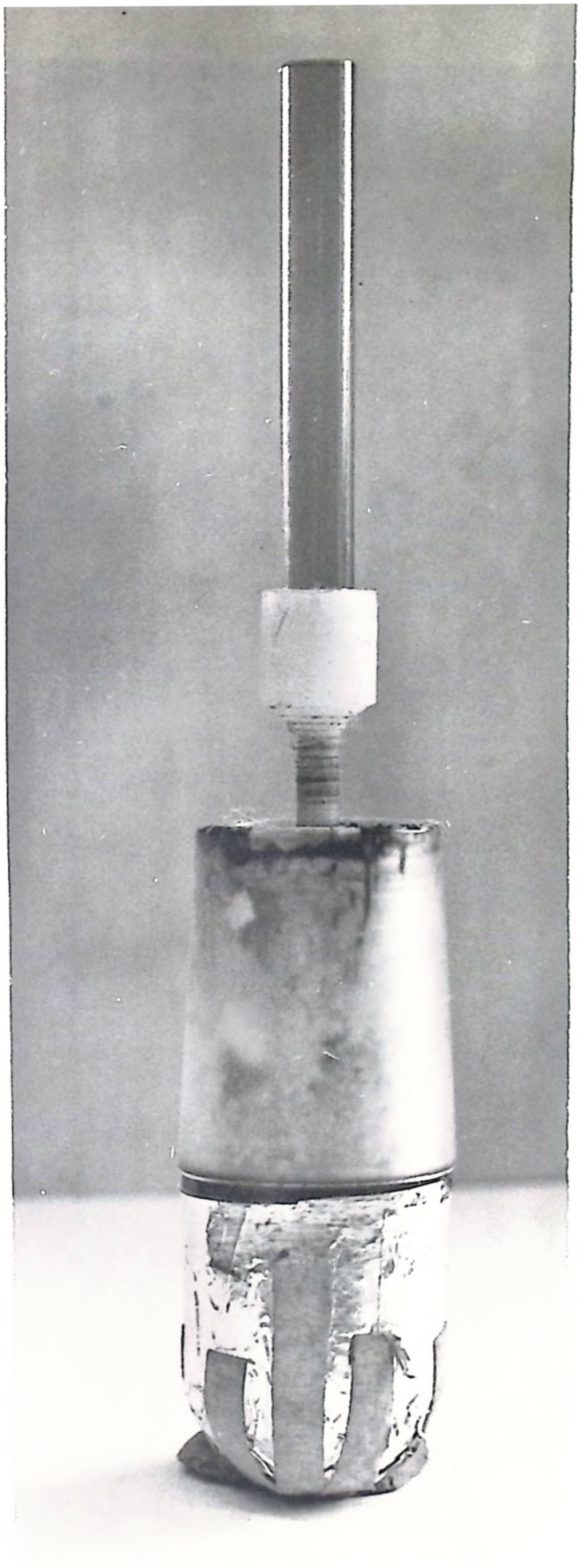

Figure 9. Ruby Crystal and Crystal Support.

The ground glass joint sealing the chamber must be made vacuum tight to superfluid helium and the vacuum grease[22] suggested was unsatisfactory as it provided a large leak to helium II on several occasions. This problem was solved by dissolving 15 parts of soap in 85 parts glycerine[23] and applying the resultant rubber solid liberally to the male portion of the ground glass joint. It is also believed the cake of soap used contained a small percentage of cold cream.

Immediately outside this chamber on a heavy paper coil form was wound the copper wire secondary. This coil was wound astatically as mentioned earlier, in the following proportions - the center portion contained 700 turns and coils on both ends contained 350 turns wound in the opposite sense, as shown in figure 11. The primary winding was also of copper and consisted of 1200 turns wound directly on top of the secondary.

Concentric with the chamber and the secondary and primary windings, the main magnet was wound. It consisted of 1392 turns of silk-covered #36 Niobium wire wound on a plexiglass coil form 1-1/4" in diameter and 3-1/4" in length. Niobium has a superconducting transition at 9°K and consumes no power below this temperature. The leads of the magnet were each bolted to a copper fin along with a #30 copper wire which carried current down from the head of the cryostat. These copper fins (one shown in figure 10) served to dissipate that heat generated from contact resistance which would otherwise reduce the current carrying capacity of the niobium in the superconducting state[24].

To maintain the constant resistance required by the mutual inductance bridge[4], the wires leading to the mutual coils were of constant resistance #36 Karma wire[4a]. These were sandwiched between two pieces

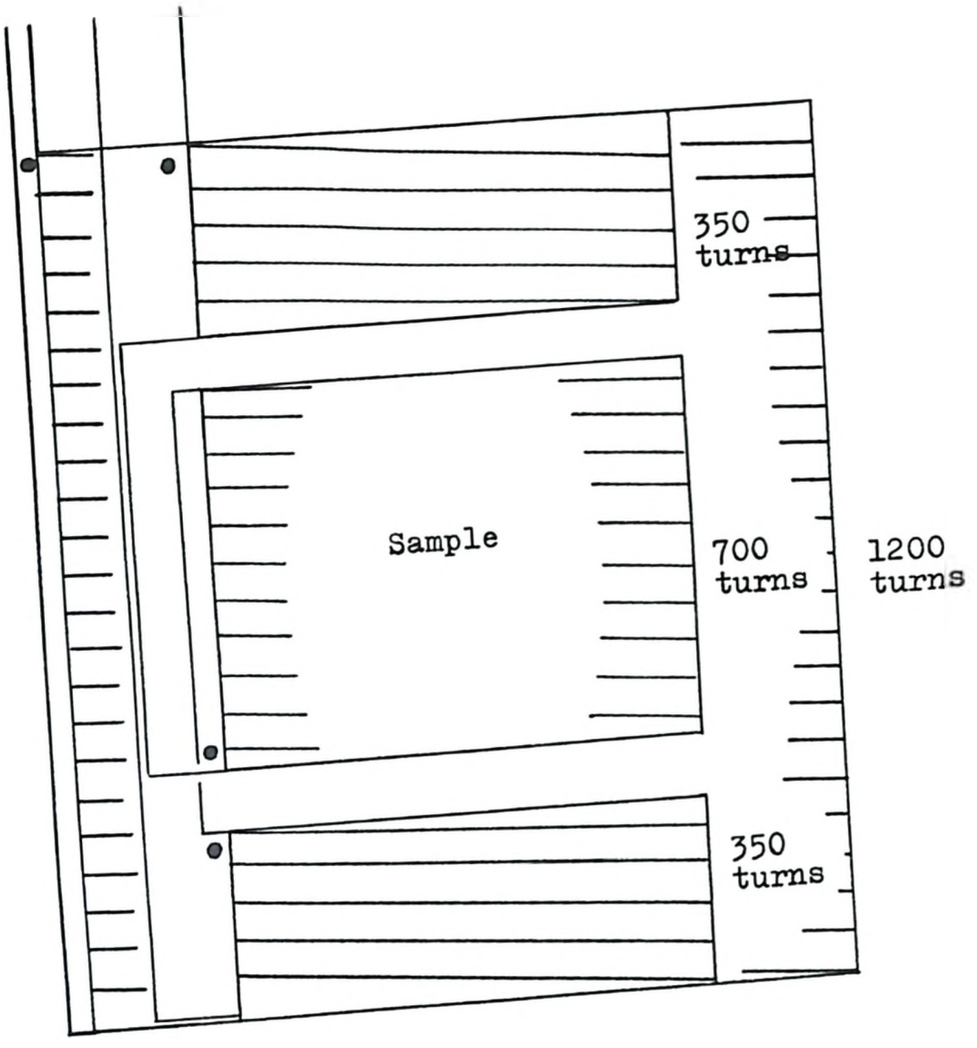

Figure 11. Mutual Transformer Schematic.

of masking tape in order to prevent electrical shorts and to keep the reactance between them constant. This is shown in figure 10. The resistance of the copper windings was constant in the temperature range of the liquid helium bath. At the bottom of figure 10 is shown, on a spiral of wire, a 1/10 watt 100 ohm carbon resistor which is used for boiling off the liquid helium at the end of an experiment.

The apparatus is now surrounded by a vacuum tight dewar and filled with liquid helium. This inner dewar is in turn surrounded with another dewar filled with liquid air and it is not made vacuum tight.

The inner dewar provides a temperature bath of 4.2°K at atmospheric pressure and to this dewar is connected a rotary pump of 2,830 liters/min. capacity. This pumping tube is shown in figure 13 as the large diameter pipe stretching to the ceiling. With this pump we may lower the vapour pressure of the helium bath and thereby lower its temperature. The pressure is kept constant over the liquid helium by means of the Cartesian Manostat shown at the lower right side of figure 12. The pressure in the low ranges (below 10 mm) is measured by the Pirani gauge shown on the top right side of figure 12 and is read on the meter behind the Cartesian Manostat in the same figure. High pressure ranges are read on the mercury and oil manometers shown in figure 13.

The high vacuum inside the chamber is provided by a 2½" oil diffusion pump shown in the center of figure 12. The pressure is measured by an ionization gauge shown at the top of figure 12 and is read on the meter mounted on the instrument rack (third instrument from the bottom). The pressure may quickly and accurately be converted to temperature by tables of helium vapour pressures[15].

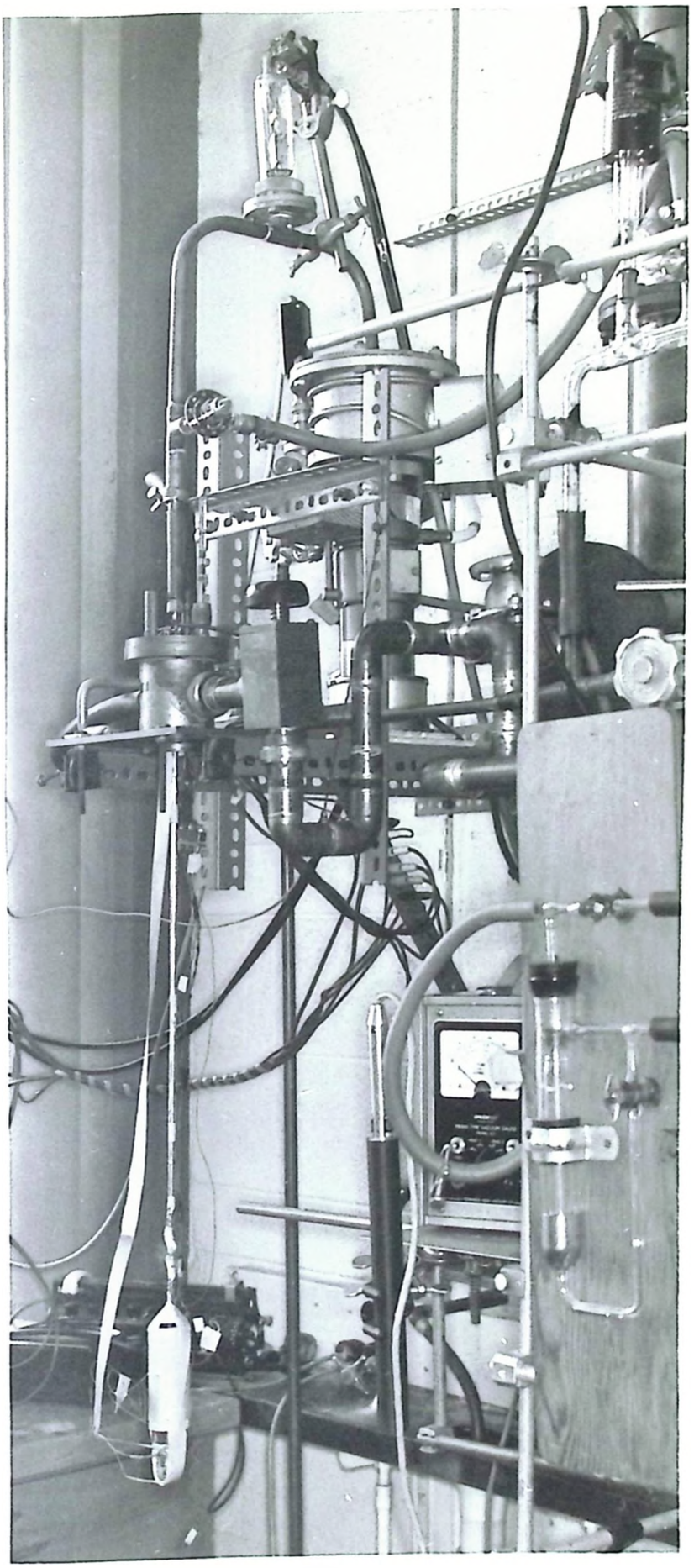

Figure 12. Chamber Vacuum Apparatus.

The rotary pump shown directly under the dewars in figure 13 is the backing pump for the oil diffusion pump.

The one kilowatt direct current power supply for the magnet is shown as the lowermost instrument in the rack and directly above it is the electronic bridge measuring the mutual inductance. A Solartron Oscilloscope is used as a null detector for the bridge.

The small power supply on the top of the rack provides power for the heater which boils off the helium and also provides heat for the circulating current operation of the magnet discussed in the following chapter. The presence of the magnetic field is detected by a Hall Effect gaussmeter mounted beside the oil manometer, and whose probe hangs beside the dewars in figure 13.

4.2 Alternate Solenoid Arrangement

In order to fulfil the proposed requirements of a circulating superconducting current in the magnet, it was necessary to place a superconducting switch across the leads of the magnet. This consisted of a coil of Niobium wire astatically wound approximately 50 times around a 100 ohm 1/10 watt carbon resistor, then covered with 5 layers of electrical insulation. Power could now be dissipated in the resistor to drive the Niobium above its critical temperature into its normal state, which in this case, means it has about 3 ohms resistance. When power to the carbon resistor is switched off the Niobium is cooled (below its critical temperature) by the liquid helium and becomes superconducting.

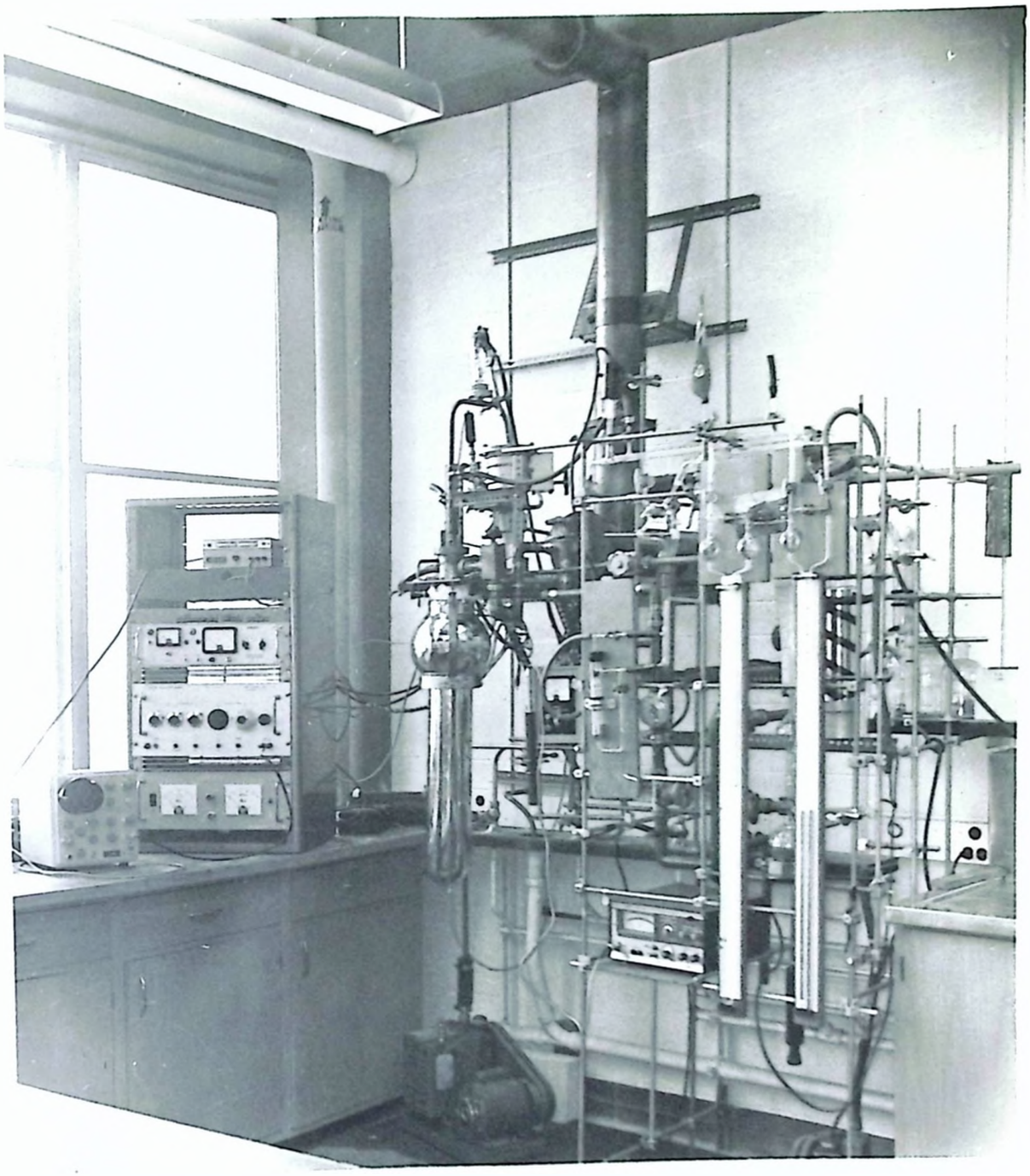

Figure 13. Complete Adiabatic Demagnetization Apparatus.

The Niobium leads to this switch were welded to the Niobium leads of the magnet by dipping the Niobium wires twisted together into a pool of mercury and applying a potential of 40-50 volts between the wires and the mercury.

To produce a circulating current in the magnet we start by supplying a one ampere current with supply #1 to the switch and magnet in parallel as shown in figure 14. Since the switch has no inductance the current will flow through the path provided by the switch. If we now increase the power input to the carbon resistor until the switch becomes normal we may drive the current through the magnet since it has no resistance. This change of path produces a field of about 500 gauss in the coil which is detected by the Hall effect gaussmeter. The output power from supply #1 is now increased until the magnet produces the required field at which point supply #2 is turned off. Power supply #1 is switched off shortly afterwards when the switch has become superconducting. The back emf generated by the magnet now encounters a zero resistance path through the superconducting switch and this current continues to flow independent of any external supply, which may then be removed.

To remove the field of the magnet, power is applied to the carbon resistor until the superconducting short returns to the normal state and the energy of the magnet is dissipated in the finite resistance provided by the switch.

In addition to having a circulating current it was desired the magnet act as the primary of the mutual bridge. The problem was solved

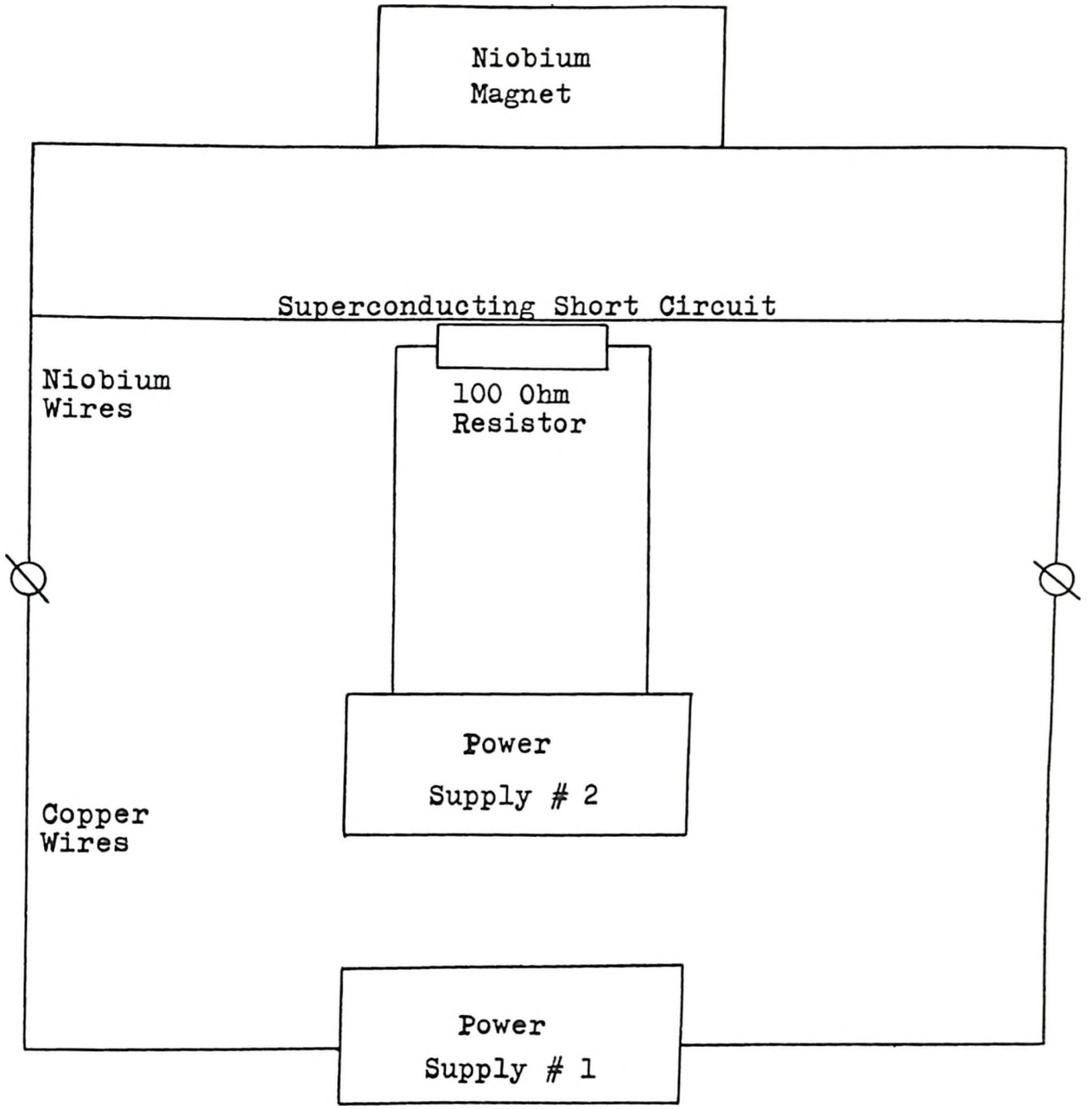

Figure 14. Superconducting Circuit.

by winding the magnet with a tap near the center such that there were two windings in series - an inner coil of about 2000 turns and an outer coil of 1000 turns. The d.c. field current flowed through these coils in series, thereby providing additive magnetic fields, but the a.c. bridge current was connected between this center tap and the superconducting short, thereby appearing as two inductors in parallel. The output from the secondary is then dependent upon the difference in coupling between each of the "primaries" with the secondary since the "primaries" are wound in opposition as shown in figure 5.

This circuit may be solved by using equations[25]

$$i_1\, jwL_1 - i_2\, jwM_{12} = i_2 jwL_2 - i_1 jwM_{12} \qquad (1)$$

$$V_3 = i_2 jwM_{23} - i_1 jwM_{13} \qquad (2)$$

Solving for i_1 from (1) and subst. into (2)

$$V_3 = i_2 jw \left(M_{23} - \left[\frac{(L_2 \neq M_{12})}{(L_1 \neq M_{12})}\right] M_{13}\right)$$

Now by approximating $L_1 = 2\, L_2$ and assuming the worse case (smallest output of secondary) to occur when the coefficient of coupling between L_1 and L_2 to be unity we have

$$V_3 = i_2 jw \left(M_{23} - (0.706)\, M_{13}\right) \qquad (3)$$

Equation (3) indicates that measuring the secondary output may not be entirely impossible in spite of the fact we have two primaries wound in opposition.

After several experiments in which no change in susceptibility was detected, this arrangement was abandoned however in favour of the apparatus outlined in section 4.1.

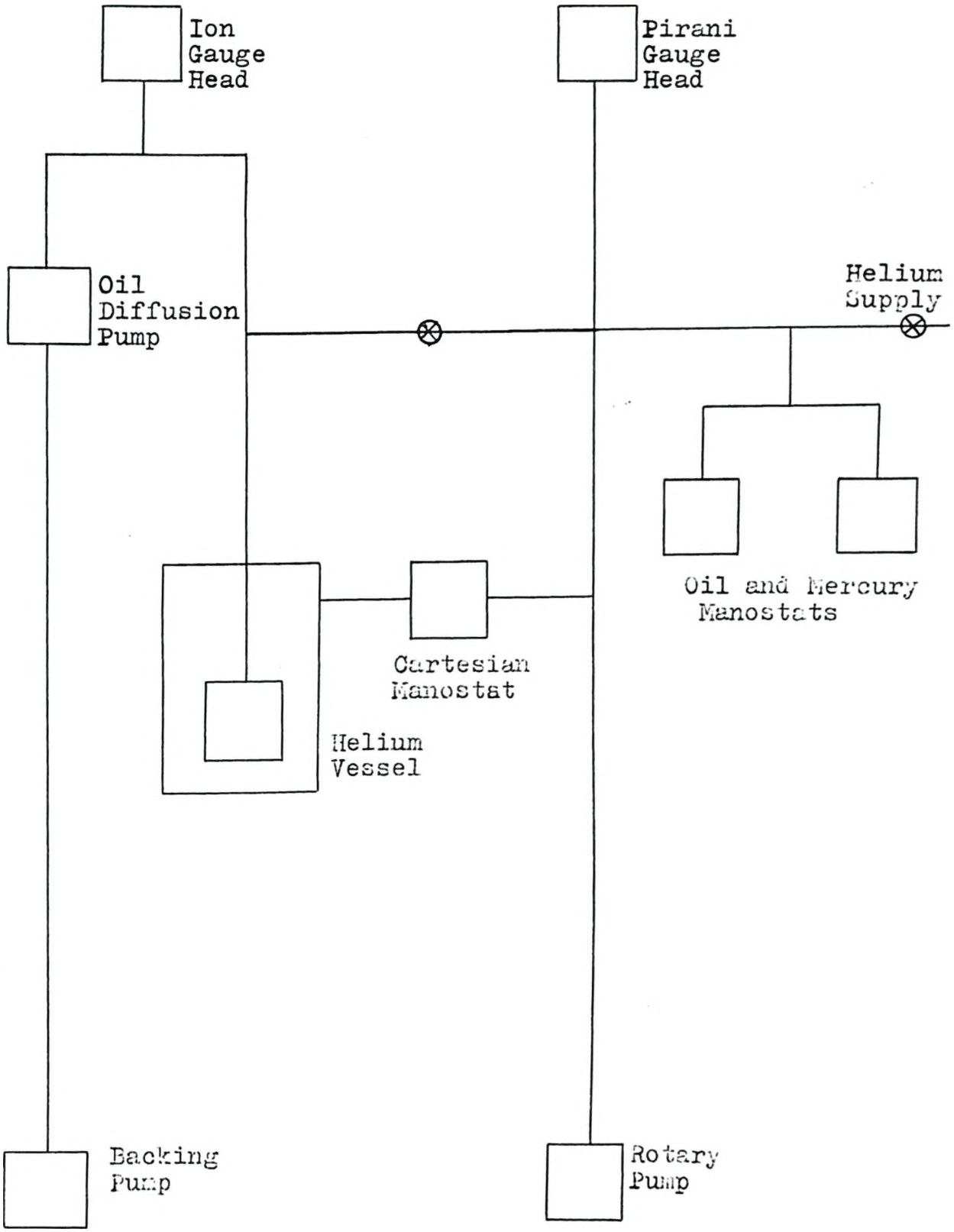

Figure 15. Vacuum system.

RESULTS

5.1 Superconducting Solenoid

Initial work was directed at building a magnet that would produce a field of approximately 4 kilo gauss. Of the magnets available in the laboratory at the time, one containing 1600 turns of niobium wound on a lucite (plexiglass) form 1 1/4" in diameter and 3 1/4" in length seemed the best suited to start the experimental work. It was found that this coil produced 200 gauss/amp and the niobium returned to its normal state at a maximum current of 5.7 amps. The addition of heat sinks as mentioned in the preceding chapter increased this critical current to approximately 10 ADC, giving a field of 2000 gauss.

To increase the field available another 1700 turns of wire was wound on top of the original magnet and the two were connected in series with the common terminal brought to the head of the cryostat for connection to the bridge. This increase in the wire turns raised the flux to 400 gauss/amp and had a critical current in the vicinity of 10-11 ADC. The resultant field of 4000 gauss was felt to be sufficient to produce cooling.

The magnet was now equipped with a superconducting switch and could carry continuous currents in the order of 10 ADC. This coil was used as the primary of the mutual bridge as described in section 4.2.

The secondary of the mutual coil was wound of copper wire as previously described and the lead wires were also copper initially.

This resulted in a great deal of confusion since the bridge measured mutual induction as a function of resistance and the resistance of copper varies by several orders of magnitude between 300°K and 4.2°K. Therefore, as the liquid helium boiled off, there was a steady drift in the mutual inductance readings that was related to the rate of exposure of the lead wires by the helium bath. This drift was large enough to mask any change of the mutual. The problem was rectified by using constant resistance Karma wires for the leads.

It was also necessary to parallel the copper lead wires of the magnet with constant resistance wire if it were additionally to be used for bridge measurements.

After several unsuccessful runs, this coil arrangement was abandoned in favor of the 3 coil system outlined in section 4.1. It was abandoned in the belief that the difference in mutual ($M_{23} - 0.7M_{13}$) was not large enough to be detected by the bridge.

The original vacuum pump used to pump out the chamber (a Welch Model 1400 - capacity 21 l/sec.) produced a vacuum of 10^{-3} mm helium at best which was permissible for a contact gas pressure but was not satisfactory for providing thermal isolation of the magnetic crystal. The addition of the oil diffusion pump provided a pressure of $2 - 4 \times 10^{-5}$ mm helium at the head of the cryostat and the chamber itself was believed to be better or at least this good. This pressure was felt to be satisfactory for isolation of the crystal.

5.2 Ferric Ammonium Sulphate

Of the paramagnetic substances available only two were chosen to attempt this experiment. The first was Ferric Ammonium Sulphate (Ferric Alum) and was chosen because of the vast amount of literature available on

this crystal[26]. The spectroscopic splitting factor for this substance is 2.00. The material itself is isotropic and therefore may be powdered and compressed into any form desired. However, the crystal decomposes at 25°C, losing its water of crystallization and consequently changing the magnetic ion concentration. The author found the decomposition was much easier to control if the sample was formed of large single crystals received from the stores and ground only roughly into the required shape with a carborundum wheel. The sample may be one or several of these larger crystals. To ensure the susceptibility could be detected, one of these crystals was placed in a special coil[27], and the mutual inductance was measured over the range 4.2°K to 1.2°K. This information is recorded in figure 16.

The jump in the mutual inductance on figure 16 as it passed through zero may be explained as a fault in the inductance bridge. Since the bridge is sensitive to resistive changes, a slight difference in switch contact resistance could produce this discontinuity when the polarity of the coils are reversed.

The other paramagnetic material used was synthetic ruby which was chosen because of its extreme chemical stability in the temperature range of interest and because its flat surfaces were ideal for depositing thin films which were to be investigated at these lowered temperatures. At low temperatures the ruby has the additional advantage that its thermal conductivity is much higher than the ferric Alum and as a result there is less opportunity for gross temperature inhomogeneities to develop. This requirement is important from temperature measurement standpoint because

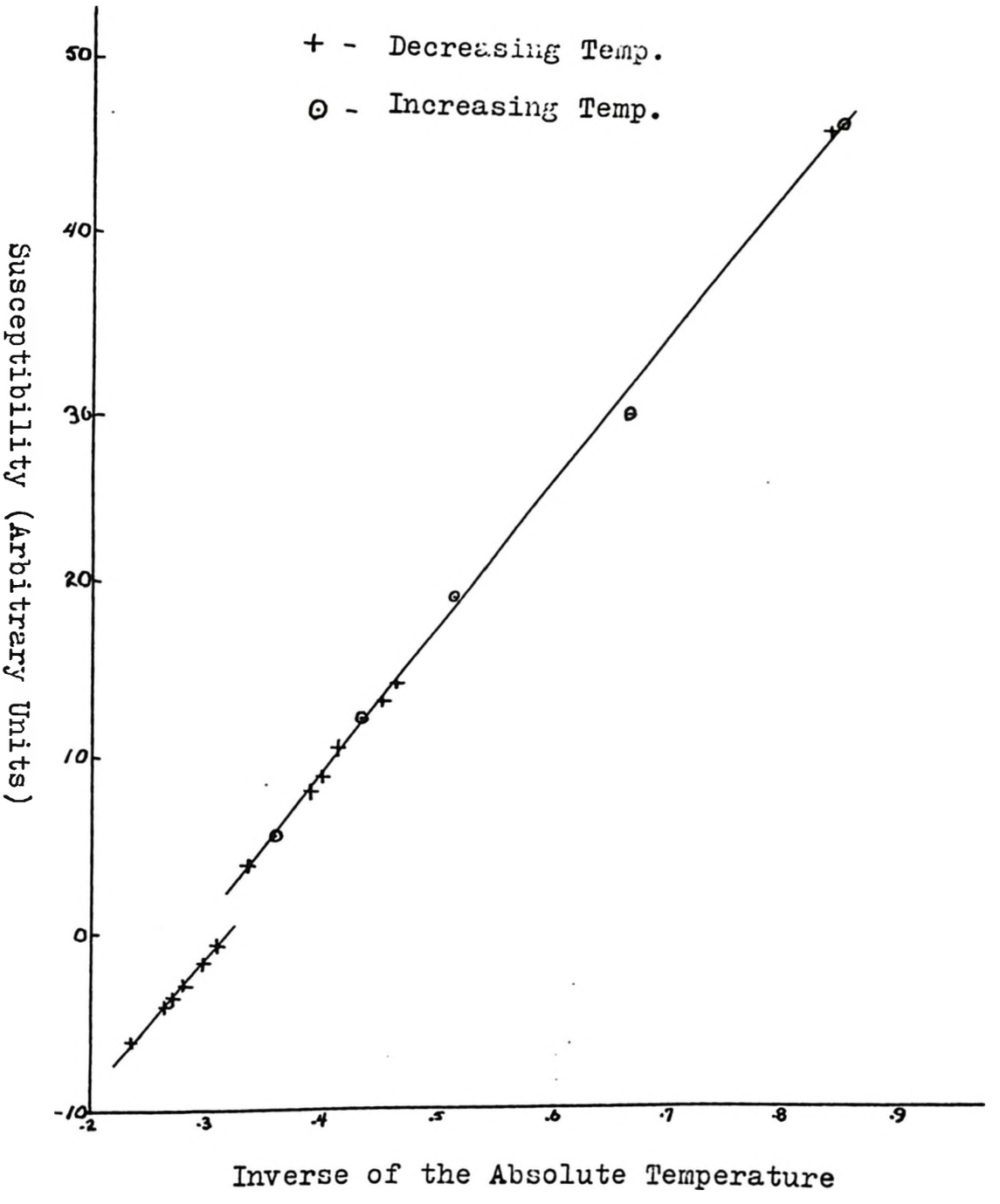

Figure 16. Susceptibility of Ferric Alum vs. the Inverse of the Absolute Temperature.

the inductance bridge measures the susceptibility averaged over the entire sample that is being cooled by the magnetic material to be at the average temperature of the material for correct temperature measurement. Ruby, because of its high thermal conductivity, ensures this is possible.

The main disadvantage to using ruby is the small concentration of magnetic ions available in the material.

Figure 17 shows the effect of isolation of the crystal of ferric Alum. At point (1), the chamber was pumped out while the temperature was being lowered and the points start to deviate from the straight line indicating that although the bath temperature is decreasing the mutual (or crystal temperature) remains constant. Therefore, it would appear we have effectively isolated the crystal in this case.

At point (2) there is a discontinuity in the curve where it was necessary to change ranges and this can also be explained as due to differing contact resistances. Helium gas at 10^{-3} mm pressure was admitted to the chamber at point (3) thereby providing contact between the crystal at a temperature of 3°K and the helium bath at 1.2°K and the crystal is cooled down to the liquid helium temperature.

At this time ferric alum was abandoned for it showed no sign of increased susceptibility upon removal of the magnetic field and in its place a sample of ruby of approximately equal weight was used.

Using the procedure outlined in section (2.2), magnetic cooling was observed in ruby. The sample was magnetized with a field of 1500 gauss for a period of 15 minutes, the last five of which the oil diffusion pump was applied to the chamber to evacuate it. In spite of the excellent

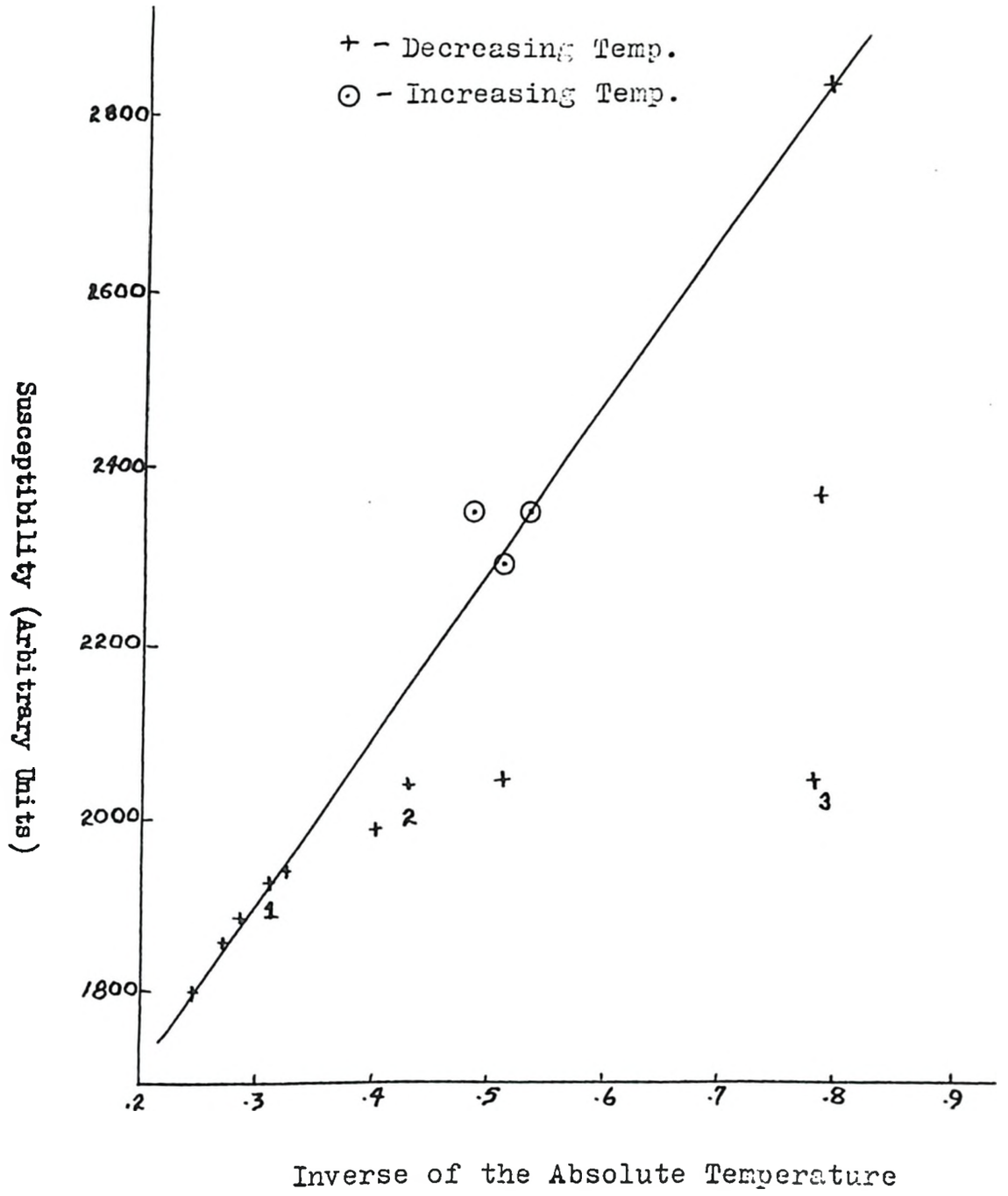

Figure 17. Susceptibility of Ferric Alum vs. Inverse of the Absolute Temperature.

vacuum achieved (2×10^{-5} mm) the sample returned to the temperature of the helium bath in less than two minutes. It is believed that the rapid temperature rise of the sample was due to radiation penetrating pinholes in the silvered walls of the chamber.

The experimental points for a run are plotted on figure 18 fitted to a simple Curie relationship. This indicates a temperature of 0.29°K was attained.

5.3 Synthetic Ruby

The ruby sample available was a crystal of Alumina 1/4" in diameter and 2" in length and containing about 0.05% by weight of Co_2O_3. The crystal because of its structural rigidity was considerably easier to mount in the demagnetizing chamber and because of its higher density was more compact and consequently easier to ensure complete thermal isolation. The ruby sample weighed approximately 5 grams as did the ferric Alum and contained 4×10^{18} chromium ion/gm[28]. This is a factor of 10^2 or 10^3 less than in the ferric Alum which is in the order of 12×10^{20} ferric ions/gm.

Since both samples were approximately the same size we would expect the mutual inductance change due to the insertion of the ruby, to be 3×10^2 less than the corresponding change due to ferric Alum.

In comparing the curves of figures17 and 18 we find the curve of ferric Alum to be 270 times greater than ruby.

Unlike ferric Alum, ruby is anisotropic, that is, the susceptibility depends upon along which crystal axis the magnetic field is

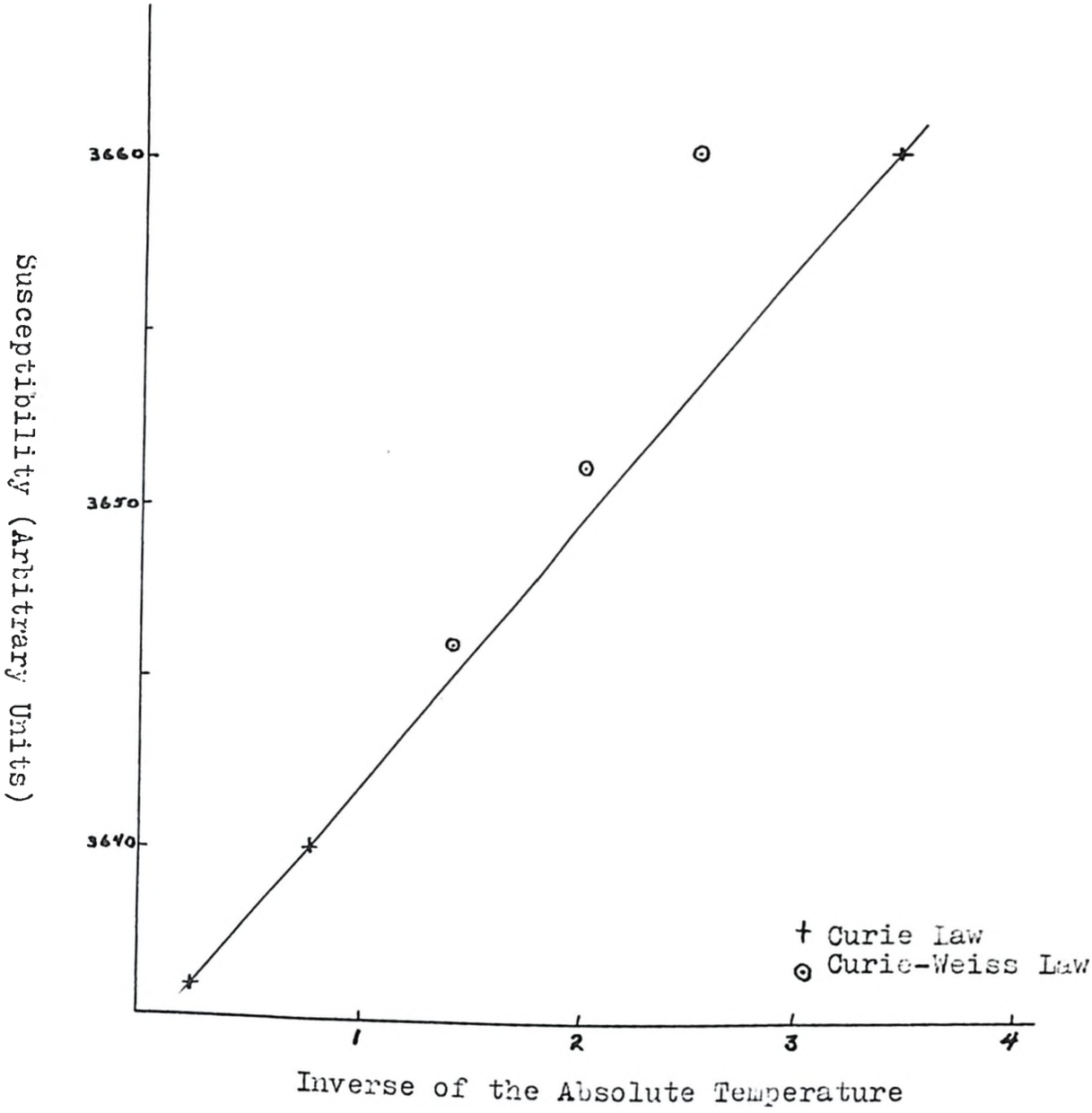

Figure 18. Susceptibility vs. Inverse of the Absolute Temperature.

applied. This particular sample was cut such that the ruby axis is parallel to the C-axis of the crystal structure. The Curie temperature in this direction is 0.214°K[29]. Therefore we must begin this problem remembering that the lowest temperature we can reach is 0.214°K.

Furthermore, we are now working in the Curie-Weiss region and the linear relationship between susceptibility and temperature can no longer be justified.

Using the Curie Weiss relationship

$$X = \frac{C}{T-0.214} \qquad (1)$$

we can compare the linear case to that given by equation (1) (see figure 18) and see the large error introduced in the Curie temperature. For example, the measured mutual inductance value of 36.600 μH would, from the simple Curie relationship correspond to an (inverse) temperature of $3.45°K^{-1}$ whereas the Curie-Weiss relationship would yield a value of $2.48°K^{-1}$. This picture is further complicated by the energy level structure of ruby which we will discuss in the next section.

The analysis of data from the ruby crystal is further complicated. Since the Cr^{+++} ion has 2 magnetic moments near the ground state (the lower one being larger than the other), then as the temperature is decreased, more ions drop to the lower energy level, consequently a higher than expected value of magnetic moment.

The upper and lower levels have spin magnetic quantum numbers +½ and +3/2 respectively[30]. Since the magnetic moment varies as the square of the quantum numbers, the upper and lower states have magnetic moments proportional to 1/4 and 9/4 respectively.

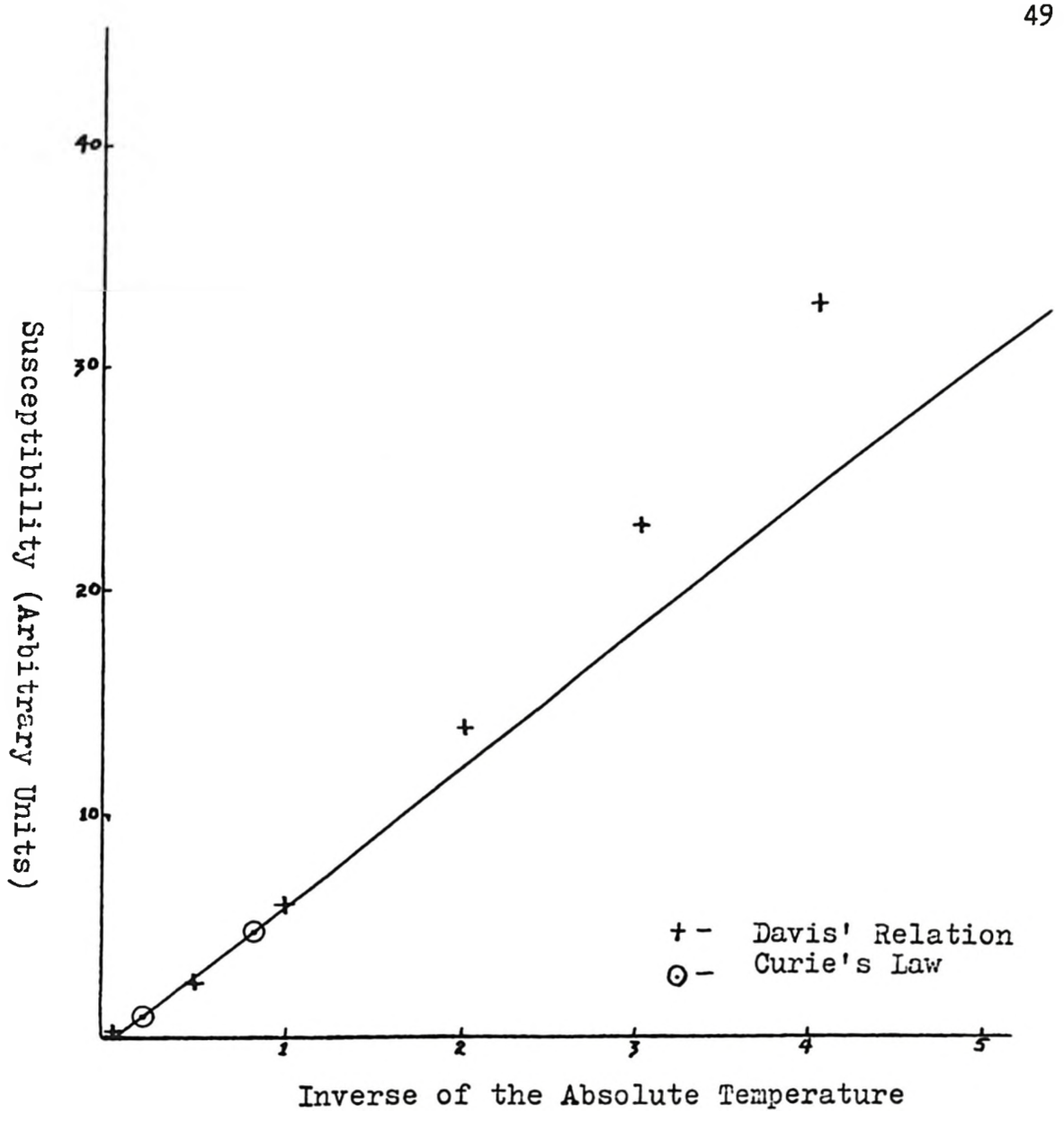

Figure 19. A Comparison of the Susceptibility given by Curie's Law and by Davis' Relation for Various Temperatures.

Consider very low temperature where all the spins are in the lowest energy state, the susceptibility expression will contain a 9/4 magnetic moment term. However, at high temperatures where the spins are evenly distributed between these 2 levels, the susceptibility expression will have a factor

$$1/2\ (1/4) + 1/2\ (9/4) = 5/4$$

Therefore as the temperature decreases the slope of the inverse temperature vs. susceptibility curve will change by a factor of 9/5.

The susceptibility may be expressed to within a few millidegrees by Davis relation[31]

$$\chi_o = \frac{N\mu_o^2}{RT} \left(\frac{9 \exp(a/kt) + 1}{\exp(a/kt) + 1} \right)$$

where N = conc. of C_2^{+++} ions/cc

μ_o = Bohr magnetor

K = Boltzman Const.

a = energy between two lowest energy levels (0.384 cm^{-1}) (33,34)

This relation is shown in figure 19 along with the simple Curie extrapolation. The temperature on the Curie law of 0.29°K gives a reading of 0.35°K on the Davis' curve.

CONCLUSIONS

The original purpose mentioned in the Introduction (Chapter 1.2) and the apparatus designed to fulfil this purpose outlined in Chapter 4.2 was abandoned because it was not possible to observe a deflection of the mutual bridge using ferric Alum in the liquid Helium range. It was first believed to be a lack of the coupling between the coils suggested in Section Chapter 4.2. To test this, the superconducting switch was removed and the mutual inductance was subsequently measured as a function of temperature by placing the primary bridge leads in parallel with the d.c. magnet supply leads with still no deflection in the mutual. At this point the apparatus was changed to the arrangement outlined in section Chapter 4.1. A new magnet was wound for the new arrangement.

Later experimentation, using the new magnet as a primary of the bridge, showed it was possible to measure the susceptibility as a function of temperature indicating that the first magnet used was defective. If we were to assume a layer of the windings on the original magnet was short circuited it would explain the results obtained and therefore does not justify eliminating the superconducting switch entirely.

However, the experience obtained from this experiment leads the author to believe that the best and most reliable arrangement would be a superconducting switch that may be burned up during the demagnetization stage. The bridge measurements would then be made by a single coil for

the primary which doubles as the magnet. Such an arrangement could only be used once on each run but is necessary because no mechanical contacts were found that were superconductive.

The ruby crystal proved to be the ultimate in chemical stability as expected whereas the ferric Alum was difficult to preserve at room temperature. The ruby could be polished until its surfaces were optically flat, providing a perfect surface on which to evaporate thin films. The concentration of the magnetic ions in the ruby was so low, however, it was difficult to measure the susceptibility. The concentration in ferric Alum was high enough to give a good measurement of the susceptibility. Better results may be obtained if the concentration of Cr^{+++} ions in Alumina is raised to approximately 0.6%. Higher concentrations result in the crystal fracturing at low temperatures[29].

Given the two substances, ruby and ferric Alum, it would appear ferric Alum is the best suited for cooling other materials to low temperatures. Since this ruby sample has a magnetic iron concentration of 10^2 to 10^3 less than ferric Alum, the heat capacity is proportionately less. The specific heat due to lattice vibration at this temperature is negligible compared to that of the magnetic spin system. The ruby on the other hand would be ideal for a thermometer since its specific heat is so low. In order that its susceptibility be more easily detected, however, its concentration of magnetic ions should be increased to approximately 0.6%.

The most convenient arrangement would appear to be a coolant crystal of ferric Alum to which is glued a smooth surface (e.g. glass) for evaporating films of the material under study. Temperature would be measured by measuring the susceptibility of the ferric Alum or by connecting the crystal of ferric Alum to a crystal of ruby by a thermal conductor, such as copper wire. We would now measure the susceptibility and relate it to temperature assuring ourselves we have made good thermal contact in all locations.

BIBLIOGRAPHY

Chapter 1

1. Simon, F.E., Kurti, N., Allen, J.F., Mendelssohn, K., Low Temperature Physics, Four Lectures, Pergamon Press, London, p. 30, 1952.

2. Woltjer, H.R., Kammerlingh-Onnes, H., Leiden Comm., No. 167, 1923..

3. Debye, P., Ann. d. Phys., 81, p. 1154, 1926.

4. Giauque, W.F., J. Am. Chem. Soc., 49, p. 1870, 1927.

5. Giauque, W.F., MacDougall, D.P., Phys. Rev., 43, p. 768, 1933.

6. deHaas, W.J., Wiersma, E.C., Kramers, H.A., Nature 131, p. 719, 1933.

7. Hader, G., Siemans-Z., 8, p. 3, 1930.

8. Arp, V.D., Kropschot, R.H., Rev. Sc. Inst., 32, p. 217, 1961.

Chapter 2

9 deKlerk, D., Handbuch der Phys., 15, p. 43, 1956.

10. Hoare, F.E., Jackson, L.C., Kurti, N., Experimental Cryophysics, p. 200, Butterworth, London, 1961.

11. Mendelssohn, K., Cryophysics, p. 23, Interscience, 1960.

12. Aelen, J.F., Shire, E.S., Nature, 139, p. 878, 1937, Proc. Cambridge Phil. Soc., 34, p. 301, 1938.

13. Kittel, C., Elementary Statistical Physics, p. 77, Wiley, 1958.

14. Casimir, H.B.G., Magnetism and Very Low Temperatures, p. 43, Dover, N.Y., 1961.

Chapter 3

15. Van Dijk, H., Durieux, M., Clement, J.R., Logan, J.K., The 1958 Helium Scale of Temperatures, U.S. Dept. of Commerce, Part 2, Monograph 10, June, 1960.

16. deKlerk, D., Steenland, M.J., Adiabatic Demagnetization, Prog. in Low Temperature Physics, Vol. 1, p. 278-279, 1955.

17. Mendelssohn, K., Cryophysics, p. 26-29, Interscience, N.Y., 1960.

18. Kurti, N., Low Temperature Physics - Four Lectures, p. 49, Pergamon, London, 1952.

19. Hague, B., A.C. Bridge Methods, 5th edition, p. 424, Pitman, 1957.

20. Pillinger, W.L., Jastram, P.S., Daunt, J.G., Electronic A.C. Mutual Inductance Bridge, Rev. Sc. Inst., Vol. 29, No. 2, p. 159-162, Feb. 1958.

Chapter 4

21. Nat. Bur. Standards, A Compendium of the Properties of materials at Low Temperatures (Phase 1), p. 3.501, Office of Tech. Services, Dept. of Commerce, Wash., D.C., 1960.

22. White, G.K., Experimental Techniques in Low Temperature Physics, p. 238, Clarendon Press, Oxford, 1959.

23. Hoare, F.E., Jackson, L.C., Kurti, N., Experimental Cryophysics, p. 132, Butterworth, London, 1961.

24. Campbell, C.K., Walmsley, D.G., Can. J. Physics, 41, p. 416, Feb. 1963.

25. Von Laue, M., Superconductivity, p. 8, Academic, N.Y., 1952.

Chapter 5

26 Casimir, H.B.G., deHaas, W.J., deKlerk, D., Physica's Grav., 6, p. 241, p. 365, 1939(a).

27 Drautman, J.J., Private Communication, April, 1964.

28 Maiman, T. et al., Phys. Rev., Vol. 123, No. 4, Aug. 1961.

29 Daunt, J., Brugger, K., Zeit. Phys. Chemie, 16-17, p. 208, 1958.

Chapter 6

30 Geusic, J. et al., Bell Sys. Tech. J., Vol. 38, No. 1, p. 291, Jan. 1959.

31 Daunt, T., Edwards, D., Kreitman, M., Pandorf, R., Snider, J., Proc. of 7th International Conference on Low Temperature Physics, 7, p. 96, 1960.

32 Davis, H.L., Zeit. Phys. Chemie, Vol. 16-17, p. 216, 1958.

33. Manenkov, A.A., Prokhorov, A.M., J. Exp. Theror. Physik, U.S.S.R., p. 28, 1955.

34 Geusic, J., Phys. Rev., 102, p. 1252, 1956.